Economic Geology
Vol. 73, 1978, pp. 1326–1365

Skarn Formation and Mineralization in the Contact Aureole at Carr Fork, Bingham, Utah

W. W. Atkinson, Jr., and Marco T. Einaudi

Abstract

Surface mapping, core logging, and compilation of underground mine maps in the Carr Fork area have led to the definition of the stratigraphic, structural, and time-space distribution of copper, copper-lead, and lead-zinc-silver ores in the western contact aureole of the Bingham stock. The succession of alteration-mineralization stages in sedimentary rocks is defined, and each stage tentatively is correlated with stages in the evolution of alteration-mineralization in the Bingham stock.

Sedimentary rocks in the contact aureole are of Pennsylvanian age and consist of quartzite with lesser amounts of calcareous carbonaceous siltstone and limestone. Compressive deformation from the southeast during Mesozoic time formed east-west trending folds and bedding plane faults across the district; differential yielding resulted in overturning of folds in the highly deformed Carr Fork area. Following the main period of folding, stress was relieved by northward thrusting; in the Carr Fork area a set of northwest-striking imbricated thrust or right-lateral strike-slip faults formed in the upper plate of the basal Midas thrust. A system of northeast-striking faults, which were later to serve as major ore solution conduits, originated largely as tension fissures parallel to the direction of maximum principal stress. Multiple intrusions of monzonite and quartz monzonite during mid-Tertiary time were controlled to a large degree by the zone of north-east faults and by steep bedding.

An Early Stage of contact metasomatism produced: diopside in quartzite and in interbedded, thin silty limestone beds; wollastonite, with minor idocrase and garnet, in thick cherty limestone; and a trace amount of sulfides. The Early Stage is related at least in part to the emplacement of the quartz monzonite of the Bingham and Last Chance stocks and continued during the initial emplacement of the quartz monzonite porphyry.

Actinolite alteration of diopside in quartzite and garnetization of wollastonite-bearing marble represent the beginning of Main Stage mineralization and are time equivalent with biotite-orthoclase alteration of igneous rocks. As the stock is approached, actinolite alteration in quartzite and hornfels exhibits textural changes from bedding streaks to orbicules and to envelopes on fractures; closer to the instrusion, actinolite is altered to biotite along fractures. Traces of pyrite accompany actinolite in the outermost zones of bedding streaks and orbicules. Chalcopyrite accompanies pyrite as the fracture filling in the envelope zones. Near the stock, molybdenite veinlets have primarily biotite envelopes. Crosscutting veinlet relations indicate that the biotite zone expanded from the stock onto the outer actinolite zone during a trend toward increasing chalcopyrite: pyrite and molybdenite: Cu-Fe-sulfide ratios. Late pyritic veinlets with actinolite envelopes represent the waning of Main Stage mineralization in quartzite.

Two cherty limestone beds, 15 to 60 m thick and separated by 100 m of quartzite, contain the major copper-bearing skarns in the district. Main Stage alteration in limestone consists of andradite-diopside superimposed on Early Stage wollastonite. Actinolite-diopside-garnet-epidote endoskarn occurs in quartz monzonite adjacent to garnetized limestone. In wollastonite, sulfides are chalcopyrite and bornite, with minor galena and sphalerite. Chalcopyrite: pyrite ratios increase from the outer edge of the andradite-diopside zone toward the intrusive contact, where trace amounts of bornite reappear. Chalcopyrite: pyrite ratios also increase with depth. Massive magnetite replaced garnet adjacent to the stock at lower elevations, and hematite is absent. At higher elevations, the skarns have a lower iron-oxide content, hematite appears, and the hematite: magnetite ratio increases to unity near the surface. These relations suggest an increase in oxidation and sulfidation states toward the surface and away from the stock.

The Main Stage of ore deposition in limestone skarns culminated in the partial destruction of andradite and diopside. Apparent reactions include: carbonation of andradite yielding calcite and quartz with hematite, magnetite, or siderite; and combined carbonation and sulfidation, yielding pyrrhotite, pyrite, and chalcopyrite in addition to calcite

and quartz. In the more diopside-rich skarn of the outer zones, alteration assemblages accompanying sulfide deposition include andradite-actinolite or actinolite in addition to the products of sulfidation and carbonation. These reactions may have been largely the result of declining temperatures; it is unclear whether any new Cu, Fe, and S was introduced at this stage.

A Late Stage of alteration produced pyrite, chlorite, montmorillonite, sericite, and talc from earlier calc-silicates and locally redistributed chalcopyrite. Lead-zinc and gold deposits, accompanied by arsenic-bearing minerals such as tennantite and arsenopyrite, also belong to this time frame. The Late Stage is believed to be contemporaneous with sericite-pyrite alteration of intrusive rocks.

The following metal zones and their maximum right-angle distances from the stock contact are recognized: (1) lead-zinc-silver northeast fissure ore (Pb/Cu = 30 to 10) in nonsilicated limestone, up to 1,200 m; (2) lead-copper northeast fissure ore (Pb/Cu = 5 to 0.2) in nonsilicated limestone, up to 900 m; (3) copper ore (Pb/Cu $\leqq$ 0.02) in garnet skarn, up to 450 m. These zones do not represent a contemporaneous zonal growth pattern but rather reflect a complex history of expansion and regression of zones dependent on rock compositions, permeabilities, and the evolution of the ore fluid.

Introduction

THE Bingham mining district, located on the east slope of the Oquirrh Mountains 40 km southwest of Salt Lake City, Utah, has produced 28.7 billion pounds of copper, lead, and zinc since the first shipment of ore in 1896. Nonporphyry ore accounts for 23 percent of this total metal production. Large-scale underground mining began in the Highland Boy copper-bearing skarn which cropped out along the western contact of the Bingham stock in the upper reaches of Carr Fork. Subsequently, lead-zinc-silver ore was mined from the Highland Boy and Yampa limestone beds in the Yampa mine, Apex mine, and others, and similar ore occurrences were developed and mined on the southern and eastern sides of the stock. Underground mining in the Carr Fork area gradually shifted to the north and to greater depths where copper ore in skarn in the Yampa limestone was followed down dip to 1,000 m below the surface. Mining terminated in Carr Fork in 1947 when the sole remaining producer, the National Tunnel and Mines Company, declared bankruptcy. The U. S. and Lark mines of the United States Smelting, Refining and Mining Company continued mining operations until 1971 and contributed more than 70 percent of the total nonporphyry ore production, primarily lead and zinc.

The Bingham mining district has been the subject of numerous geological studies, the emphasis of which has shifted with exploration and mining. The early papers of Hunt (1924), Winchell (1924), and Lindgren (1924) dealing with the mineralized sedimentary rocks of the western contact zone followed the early mining developments in that area. Since 1924, the majority of studies have concentrated on the disseminated copper ore in intrusive rocks. Recent investigations by Stacey et al. (1967), Rubright and Hart (1968), and Field and Moore (1971) deal with lead-zinc ores in fissure and replacement deposits, but the skarns largely were ignored until Atkinson (1975), Einaudi (1975a), and Reid (1975) presented short notes on various aspects of skarn geology at the S.EG. Bingham Field Conference. The present paper documents in greater detail some of these recent studies of the western contact zone of the Bingham stock.

The first portion of the present study describes the stratigraphy and structural setting of the western portion of the district. Emphasis is placed on synthesis of district structure based on new data acquired from deep drilling by the Anaconda Company and recently published accounts. The second portion of the paper describes and interprets the mineralization and alteration of limestone, calcareous quartzite, and thin interbedded limestone in the contact aureole on the northwest side of the Bingham stock. Contact effects are separated into three stages based on age relations and distribution of characteristic assemblages: (1) an Early Stage of contact metasomatism which resulted in the formation of diopside-, wollastonite-, and quartz-bearing assemblages near the stock, and tremolite, talc, dolomite, calcite, and quartz farther out, accompanied by little or no sulfide deposition; (2) a Main Stage of copper ore deposition accompanied by actinolite- and andradite-bearing assemblages; (3) a Late Stage of pyritic mineralization accompanied by montmorillonoids, talc, chlorite, and carbonates.

A careful study of over 30,000 m of drill core was the principal method of investigation, with primary emphasis on details of structure and mineralogy. Selected samples were studied by X-ray diffraction and in thin section in order to confirm hand-lens identification. Logging was carried out at a scale of 1″ = 20′ and, locally, at 1″ = 10′ where complex relations warranted. Some surface mapping was done

at a scale of 1″ = 100′. The area studied measures roughly 2 km perpendicular to the northwest margin of the Bingham stock and about 3 km parallel to it. The vertical range is about 2,000 m, represented by the depth of the deepest drill holes.

Geologic Setting

Sedimentary rocks

The Oquirrh Basin, which covers approximately 60,000 sq km in north-central Utah, is a unique basin containing an unparalleled thickness of sedimentary rocks when compared with the same time period elsewhere in North America (Roberts et al., 1965). The basin accumulated approximately 8,000 m of fine-grained sandstones, siltstones, and limestones of shallow to intermediate depth marine water origin from Late Mississippian through Early Permian time. Internal sedimentary structures suggest source areas to the north, northwest, and northeast. The shelf margin was located about 80 km east of the present site of the presumed basin center, and the thickness of time-equivalent shelf strata is only 900 m (Tooker and Roberts, 1962).

The middle part of the Oquirrh Group, locally designated the Bingham Mine Formation (Fig. 1), is of early Missourian age and rests upon middle Des Moinesian strata of the Butterfield Formation. The Bingham Mine Formation consists predominantly of fine-grained quartz sandstone commonly quartz-cemented to orthoquartzite, with lesser amounts of interbedded dark gray carbonaceous limestone and calcareous carbonaceous siltstone. Limestone is more plentiful in the lower 600 m and comprises approximately 12 percent of the total volume. Two basal limestone members, the Highland Boy and Yampa (known as the Jordan and Commercial on the east side of the Bingham stock) are the thickest and most extensive carbonate units and constitute the only major ore-bearing horizons of the western contact zone.

Limestone: Limestone in the Bingham Mine Formation is thin to medium bedded, consisting of fine- to medium-grained bioclastic calcite grains cemented by finely crystalline calcite. Minor amounts of carbonaceous material, usually less than 1 percent organic carbon by weight, are pervasively distributed throughout the matrix, and color the fresh limestone gray to black. Zones of coarse fossil debris are present in many of the limestone beds.

Bedded and nodular chert is present in some of the limestone beds and is especially characteristic of the Highland Boy and Yampa members. Most of the chert formed by replacement and preserved the original bioclastic texture of the replaced calcite. Replacement chert nodules grade from incipient, with only an external shell of fine-grained quartz surrounding limestone, to complete, with most of the chert being intermediate between the two types.

Nearly all limestone beds contain significant amounts of clastic quartz, and gradations from slightly sandy or silty limestone to limy sandstone or siltstone are present throughout the formation. A general correlation between quartz grain size and quartz percentage has been noted: beds containing less than 15 percent clastic quartz nearly always contain predominantly silt to very fine grained sand-sized particles, whereas higher quartz percentages are assocciated with larger quartz grain sizes from 0.2 to 0.5 mm. Rapid lateral variation in quartz content and grain size within individual beds is common in the upper one-third of the Highland Boy and Yampa limestone members. Quartz sand lenses or thin sandstone interbeds alternate with pure limestone beds near the tops of the members, resulting in a gradational hanging-wall contact, in contrast with the generally abrupt lithologic change at the footwall. This latter feature is well illustrated by Winchell (1924, fig. 1).

Isopach studies of the Highland Boy, Middle Quartzite, and Yampa members indicate east to northeastward thinning from Middle Canyon (located 5.5 km SW of Carr Fork) to the Bingham district. Observed thicknesses of the Yampa and Highland Boy limestones in the axial portions of the Rood and Apex folds are two to three times normal stratigraphic thickness. These excess thicknesses could be due to flowage toward the hinges of the folds, or possibly to low-angle faulting within the Yampa limestone.

Siltstone: Siltstone of the Bingham Mine Formation is intimately associated with the limestone members but also occurs interbedded with quartzite. Siltstone beds are thin to medium bedded, 20 cm to several meters thick, and moderately to very calcareous. They invariably contain minor amounts of carbonaceous material and are locally cherty and fossiliferous. Siltstone is known to grade laterally into limestone or sandstone, and thus represents a transitional facies between the two end-member types. Siltstone comprises approximately 5 to 10 percent of the Bingham Mine Formation in the Bingham district.

Quartzite: Orthoquartzite or sandstone, light tan to light gray in outcrop, is the dominant lithology in the Bingham Mine Formation, comprising approximately 83 percent of the total. Quartzite is thin to medium bedded, parallel to cross-bedded, often cross-laminated, and locally contains contorted bedding. It is bimodal and well sorted, having a silt fraction and a fine- to medium-grained sand fraction and is

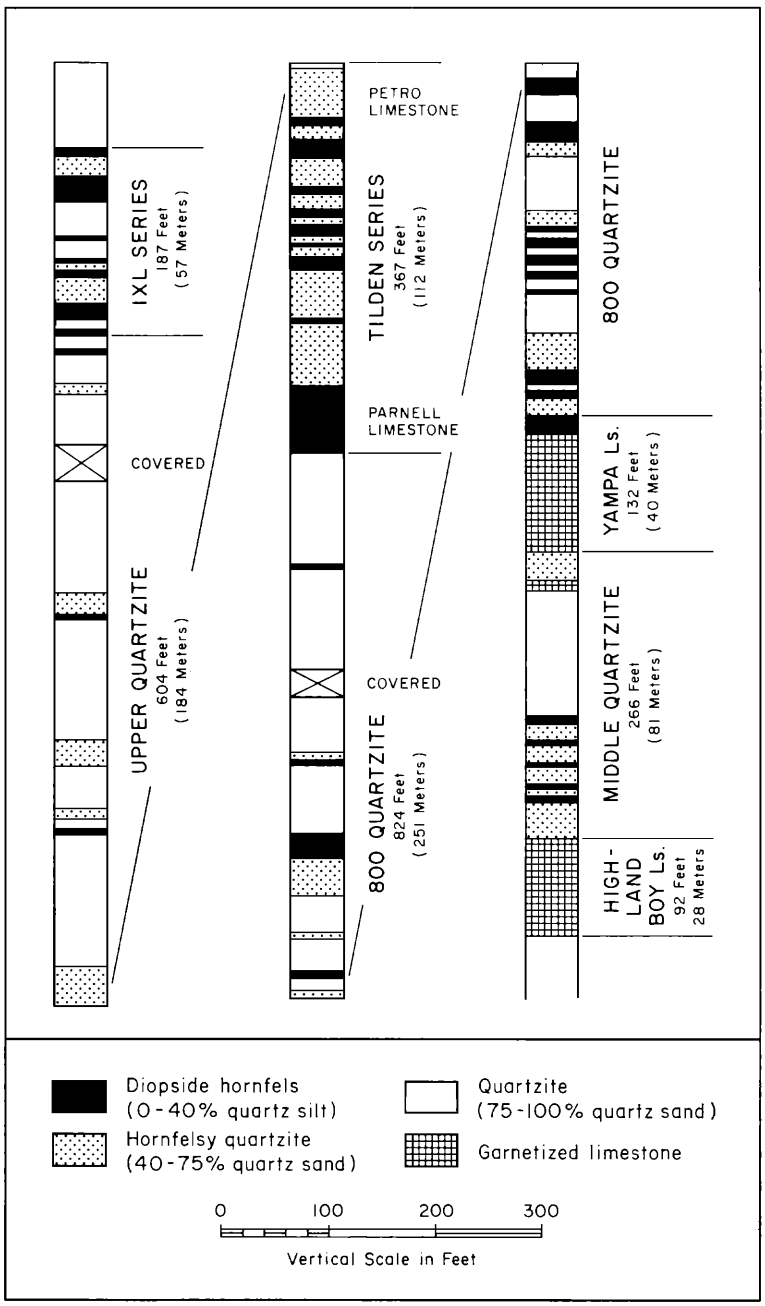

FIG. 1. Stratigraphic section of a portion of the Bingham Mine Formation of the Oquirrh Group. Section including Highland Boy and Yampa limestone members is based on surface drill holes in Carr Fork; section from top of Yampa to base of Tilden series was mapped on 6190 bench, Utah Copper pit; upper portion was mapped on surface exposures in Carr Fork.

remarkably pure, averaging greater than 60 percent quartz grains with generally small amounts of feldspar (microcline and sodic plagioclase) and heavy mineral grains. Rounded clastic calcite grains comprise the remainder. Rarely in a few thin beds as much as 20 percent clastic microcline was noted. Cementing material consists of quartz overgrowths, calcite, and small amounts of chalcedony. A mixture of quartz and calcite cement often is found in the same sample.

The majority of foresets of cross-laminated sandstone and quartzite dip to the south, indicating a

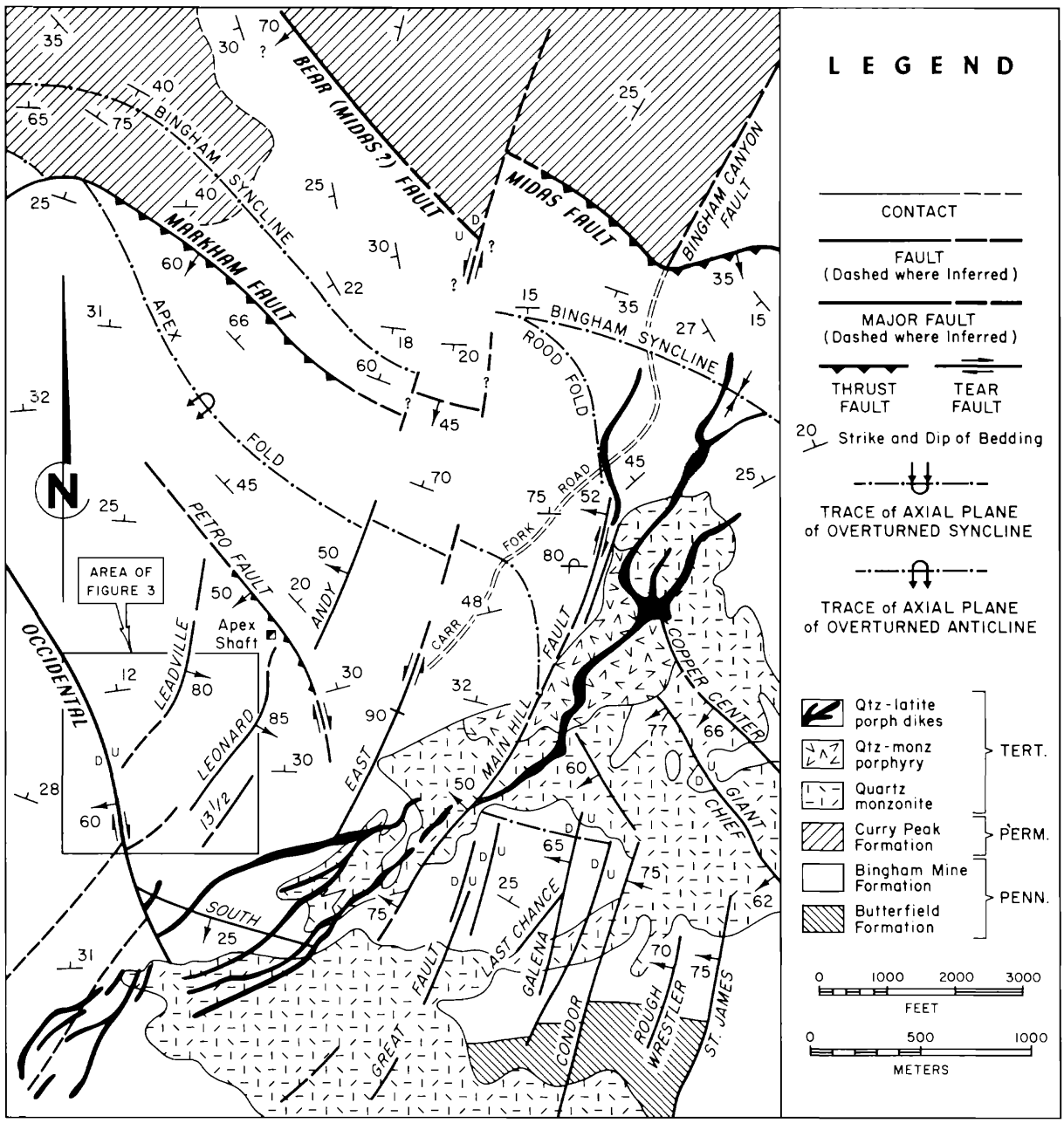

FIG. 2. Simplified surface geologic map of the west-central portion of the Bingham district. Geology of Kennecott property based on Kennecott maps (field trip map distributed at Cordilleran G.S.A. Meeting, 1970; plate 2, Guide Book to the Bingham Mining District, 1975).

northern source of sediment. Peneconsolidation slump structures also indicate that the topographic low or basin area was to the south.

Shale partings: Shale partings, paper thin to 2 cm in thickness, occur throughout the section. They are most common at the bases and tops of limestone and siltstone beds and occur with variable frequency through quartzite. They range in abundance from as many as 25 per m to as few as 1 per 15 m. Shale partings in general indicate true bedding attitudes and are useful for structural interpretations in thick sections of cross-bedded quartzite. The shale consists of illite, montmorillonite, and fine quartz, with minor amounts of carbonaceous matter and pyrite.

Structure

New information gained from deep drilling, combined with surface mapping and re-examination of underground mine maps, has resulted in a structural interpretation which differs in some respects from

previously published accounts (Roberts and Tooker, 1961; James et al., 1961; Tooker, 1971). The pre-Tertiary structure played an important role in determining the configuration of igneous rocks and the geometry of orebodies in the sedimentary rocks of the contact aureole and hence is discussed in some detail in this section.

Sedimentary rocks of the district yield evidence of numerous periods of deformation, although the dominant structural pattern was acquired during the Sevier orogeny of Cretaceous age (James et al., 1961; Tooker, 1971). The fault pattern is dominated by a set of northwest-striking, moderately southwest dipping faults, and a set of northeast-striking, steeply dipping faults (Fig. 2). These faults, and west-northwest-striking folds which they cut, formed in the upper plate of the Midas thrust, which is thought to be one of numerous imbricated structures of the basal Charleston-Nebo thrust (Roberts et al., 1965; Tooker, 1971). Subsequent faulting during intrusive events of middle Tertiary time and Basin and Range faulting appear to have occurred along Cretaceous structures. The major structural features of the district are discussed below in apparent formative sequence.

Folds: Pennsylvanian strata in the southern half of the Oquirrh Mountains are folded into long, arcuate, northwest-trending anticlines and synclines whose axial planes are overturned to the northeast (Boutwell, 1905; Gilluly, 1932). These folds are thought to represent the initial stages of deformation caused by thrusting from the southwest (Roberts and Tooker, 1961).

The Bingham syncline passes through the northern portion of the district. Beds on the northern limb dip 20° to 35° W to SW, whereas those in the southern limb dip 15° to 50° N to NW. The relatively uniform dip of beds in the southern limb is abruptly disturbed within a northwest-trending zone of steep to overturned bedding which passes through the center of the district (Fig. 2). The northern and southern limits of steep beds define a syncline (Rood fold) and an anticline (Apex fold), respectively, whose axial planes are sharply overturned to the north. The Rood fold plunges 20° WNW, whereas the Apex fold is essentially horizontal. Thus, the amplitude of vertical bedding decreases from west to east, and the zone pinches out in the eastern portion of the district, southeast of the Bingham stock. An eastward decrease in folding intensity is also displayed by the Bingham syncline, which becomes broad and ill defined east of Carr Fork-Bingham Canyon.

The axial plane of folds is often the locus of intense fracturing in quartzite (James et al., 1961) and overthickening of limestone beds.

Bedding plane faults: Significant bedding plane faults, which presumably became active during folding, formed largely at the base of limestone beds where abrupt lithological changes occur (Hunt, 1924). These faults are especially prevalent in the area of gently northwest dipping beds in the eastern portion of the district, northeast of the Giant Chief and Copper Center faults, where much of the slippage may have occurred during movement on the Midas thrust fault (Smith, 1975). Gently north dipping bedding faults on the footwall of the Yampa limestone in the southern portion of the Carr Fork area display northward dip-slip movements of 150 to 450 m (Farmin, 1933; Rubright and Hart, 1968). Farther north, bedding faults are also common at the base of the Lark and Highland Boy limestones. The importance of bedding faults during hydrothermal activity in Tertiary time is illustrated by the abnormal concentration of sulfides in such structures; the Lark lead-zinc vein on the east side of the district and the Yampa footwall copper vein in the Yampa mine on the west side are outstanding examples.

Northwest fault system: A series of prominent faults strikes northwesterly across the district, subparallel to the fold axes. Near the surface and west of Carr Fork-Bingham Canyon, these faults dip 50° to 60° SW. To the southeast they either swing to a southerly strike and merge into the northeast fault system or flatten and merge with bedding plane faults. All the northwest faults offset folds and appear to have an early, probably Cretaceous age, reverse or right-lateral component of movement. The majority also have a later, Tertiary, Basin and Range component of normal movement; this is especially clear for the Occidental fault.

The major northwest faults include, from north to south, the Midas, Bear, Markham, Copper Center, Giant Chief, Petro, and Occidental faults (Fig. 2). The Midas is a major thrust fault which dips 20° W in the Lark mine and 40° to 60° SW on the west side of Bingham Canyon. According to James et al. (1961), sedimentary rocks in the footwall are completely folded and the style of folding bears little resemblance to that of the upper plate. Stratigraphic offset varies from 0 to 1.6 km due to the vagaries of folding; the net movement has not been determined. Roberts et al. (1965) believe that the Midas is a fault of regional importance; however, Smith (1975) suggests that the Midas is restricted to the district and, toward the east, swings to a southerly and then southwesterly strike and merges with bedding faults. The Bear fault, a steeply dipping reverse fault in the northern portion of the district, may represent the westward continuation of the Midas fault (James et al., 1961).

The Markham fault was first defined by deep drilling in 1970. It crops out 1,000 m southwest of

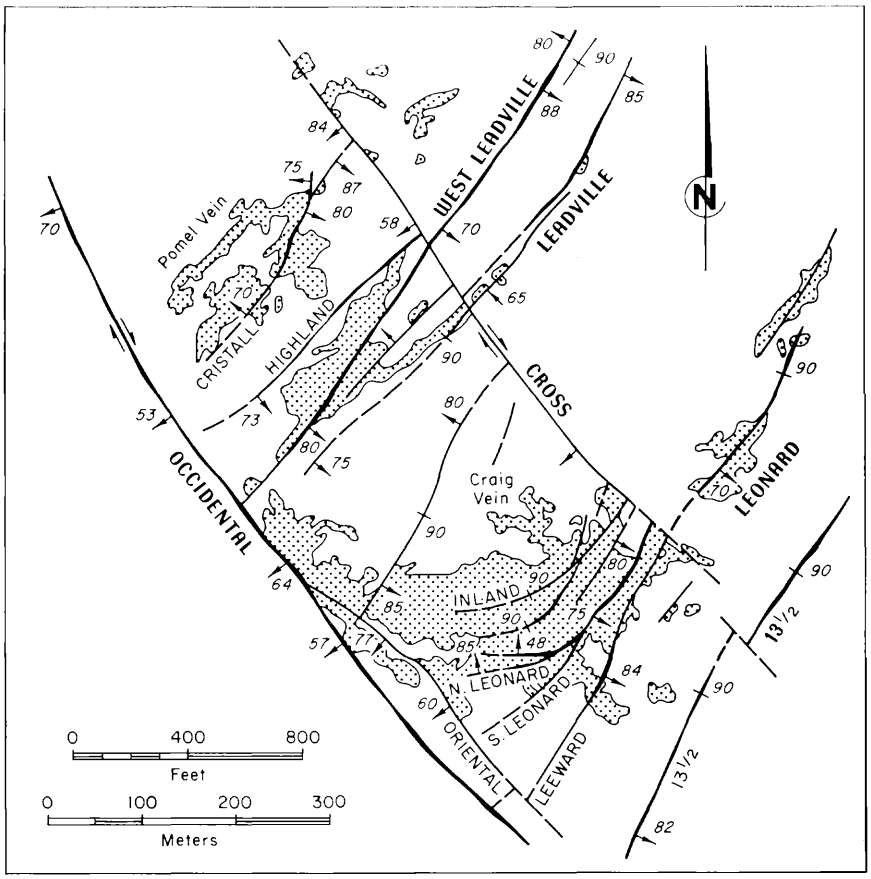

FIG. 3. Faults, fissures, and Pb-Zn-Ag stopes (stippled) on the footwall of the Yampa limestone in the western portion of Highland Boy mine, Carr Fork, projected onto a horizontal plane; 7,400- to 7,600-ft elevation.

the Midas fault, strikes N 70 W, and dips 55° to 65° SW. At depths of 1,000 m the dip of the fault flattens to 45°. Stratigraphic offset, indicating reverse movement, decreases from 500 m on the west to 180 m on the east over a distance of 600 m within the area of deep drilling. The Markham fault has not been recognized on the east side of the Bingham stock, although with a slight change in strike it projects into the Giant Chief fault (Fig. 2). Smith (1975) has described the latter as a right-lateral tear fault separating gently northwest dipping beds on the north from steeply north dipping beds on the south. Some right-lateral movement associated with the Markham thrust fault may also have been taken up by the Great-Main Hill fault zone (Fig. 2).

Other faults which have the same general attitude as the Bear-Midas and Markham-Giant Chief faults, and which may be of similar origin, include the Petro and Occidental faults. The Petro fault strikes N 45° W and dips 45° to 60° SW in the Apex mine and likewise at the surface near the Apex shaft. The Occidental fault, located on the southwest side of the district, strikes N 25° W and dips 55° to 70° SW. A review of underground maps of the Utah Delaware and Utah Metals mines suggests that the Occidental fault originated during Cretaceous thrusting as a right-lateral tear fault and that subsequent normal movement occurred during Basin and Range faulting.

Although the northwest faults are the most significant faults in the district in terms of displacement and continuity, they are only weakly mineralized where they intersect limestone beds. The lack of major orebodies, which are present along bedding faults and northeast-striking faults, suggests that the northwest system was relatively impermeable, presumably due to its development under compressional stress.

Northeast fault system: The most important mineralized fault system in the district consists of nearly vertical, northeast-striking faults which commonly display little or no evidence of offset. The attitude and spatial distribution of these faults suggest that

they originated during folding and thrusting and later were reactivated by intrusive activity.

The possibility that the northeast faults represent, in part, a set of conjugate shears related to northwest right-lateral faults is illustrated by the apparent left-lateral offset and drag of the Yampa limestone on the Andy and Yampa faults in the Apex mine (Hunt, 1924, fig. 4) and the 100 m of left-lateral movement on the East fault. However, because the majority of northeast faults show negligible offset, they appear to have originated largely as tension openings.

The northeast faults are abundant near the crest and in the southern limb of the Apex fold, a relation which Tooker (1971) interpreted as resulting from release of tension during arcuate folding. An additional possibility supported by fault relations in the Highland Boy mine (Fig. 3) is that the northeast fissures represent tension fractures related to rotational shear on northwest faults, with the principal regional stress oriented approximately north-south. Such a mechanism would explain the lack of continuity and abrupt changes in abundance of northeast fissures across northwest faults, as illustrated in Figure 3.

The northeast fault system was the dominant structural control for fissure and replacement Pb-Zn-Ag ores south and west of the stock (Figs. 3 and 17). This fault system undoubtedly served as a major locus of circulating hydrothermal fluids during the Late Stage of alteration and mineralization; it guided not only Late sulfide mineralization in unaltered limestone but also Late sulfides and retrograde alteration of Early skarn and hornfels. The influence of northeast faults on the early development of skarn is unknown due to the pervasive nature of early silication.

Summary and relation to regional structure: The structural configuration of the Bingham district, as revealed through mining exposures and deep drill holes, shows evidence of differential movement of numerous blocks on steep, trough-shaped thrust faults which may be interpreted as the imbricated distal ends of flatter thrust faults at depth. As suggested by Tooker (1970) with respect to the Cordilleran overthrust belt as a whole, differential movement was facilitated by tear faulting, imbrication, and overfolding. This occurred on a local scale at Bingham, and the apparent direction of movement was north-northeasterly as opposed to the dominant easterly direction for the thrust belt as a whole.

During the Mesozoic orogeny, the site of the Bingham district was located astride the Cortez-Uinta axis, an east-west-trending belt that had undergone uplift and faulting during Early Ordovician and again in Late Devonian time and which persisted as a highland during Pennsylvanian and Permian sedimentation (Roberts et al., 1965). Irregularities in this east-west highland may have been translated into local deflections of over-riding thrust planes during Mesozoic time and resulted in an increased complexity and density of faulting and fracturing relative to areas lying north or south of the axis. The Cortez-Uinta axis, representing a fundamental zone of crustal weakness, localized igneous activity in mid-Tertiary time.

Igneous rocks

Localization and configuration: Butler et al. (1920) were the first to suggest that the Bingham intrusions represented a westward continuation of the Uinta arch, and this concept was later emphasized by James et al., (1961). More recently, numerous authors (Zietz et al., 1969; Tooker, 1971; Stewart et al., 1977) have underscored the strong correlation between (1) the location of the Cortez-Uinta axis as defined by Roberts et al. (1965) on the basis of Precambrian and Paleozoic stratigraphic and tectonic history, and (2) the presence of 27- to 39-m.y.-old calc-alkaline stocks, associated mineral deposits, and aeromagnetic highs in a belt 80 km long from Stockton to Park City. Thus, the Bingham porphyry copper deposit appears to be a good example of lineament control. It is intriguing, however, that on a district scale there is little or no evidence for an east-west structural grain, and the configuration of the stock largely is controlled by bedding attitudes and northeast-striking faults.

The bulk of the Bingham stock was emplaced east of the Great-Main Hill fault zone in an area of unusually well developed northeast fissures. James et al. (1961) have suggested that the zone of intersection of these northeast fissures with the northwest faults, particularly the Bear and Occidental, was a fundamental control, and have emphasized the cross-cutting relation between igneous contacts and sedimentary bedding. However, recently acquired data suggest a different interpretation: the stock appears to have been localized by northeast fissures and areas of steep bedding. The general conformity between intrusive rocks and bedding is particularly well illustrated near the surface along the southern and western contacts of the stock where the quartz monzonite was emplaced along steep bedding in the northern limb of the Apex fold. South of the Apex shaft, the intrusive follows the footwall of the steeply dipping Yampa limestone over a vertical interval of 1,000 m. At greater depth along the western contact, drilling has revealed that the intrusive contact is a nearly planar surface which strikes N 40° E and dips

58° NW; this surface is parallel to and on projection with the Great-Main Hill fault zone, which presumably was active during intrusive activity. The contact is only slightly discordant with the attitude of sedimentary rocks at depth, and this low angle of intersection was partly responsible for the unusual areal extent of skarns. The northern and eastern contacts of the stocks are interpreted by E. C. John (pers. commun., 1976) as having been controlled by steeply dipping limestone beds in the footwall of the Midas thrust; the stock cut through the thrust and maintained its steep attitude on the east side as it crosscut more gently dipping beds in the upper plate of the thrust. The location of northwest faults such as the Bear-Midas and Occidental relative to the stock apparently is a coincidence of the level of erosion; the dominantly steep stock cuts these relatively flat structures. The northwest faults are characteristically tight and did not present avenues for migration of magma or hydrothermal fluids. This role was reserved for the steeply dipping northeast fault system, which guided not only the early intrusives but also the late quartz latite porphyry dike swarms (Fig. 2).

Rock types: Only minor exposures of igneous rocks are present in the Carr Fork area, but numerous vertical drill holes encountered igneous rock at depth. In general, observations of drill core agree closely with descriptions of igneous rocks given by Stringham (1953), Bray (1969), and Moore (1973).

Quartz monzonite, the earliest phase of the Bingham stock, occurs in small bodies locally along the northwestern edge of the stock, north of the Apex shaft. In many cases, a few meters of this rock were encountered in drill holes just above quartz monzonite porphyry. It also occurs as sills and small dikes, particularly at the bases of the major limestone beds adjacent to the stock, and as extensive bodies south of the Apex shaft. The quartz monzonite is equigranular, with an average grain size of 1 to 2 mm. In some specimens, fresh K-feldspar is pale pink and polysynthetic twinning is visible on cleavage surfaces of plagioclase. However, the identity of the feldspars generally is obscured by alteration, and their prealteration proportions could not be estimated in hand specimen. Biotite occurs as irregular clots of very fine grains, medium to dark brown in color. In some intervals, sparse pink K-feldspar crystals up to 1 cm in diameter were noted.

Quartz monzonite porphyry, the second intrusive phase, forms the bulk of the stock adjacent to the deep Carr Fork skarn. The porphyry is a large, dikelike mass, about 300 m thick and 1,000 m long (see fig. F-2, John, 1975), which strikes N 45° E and dips 50° NW. The thickness of the dike at depth is confirmed by one drill hole which encountered a significant interval of quartzite on the lower side. Porphyry also occurs in numerous small dikes near the contact of the stock at depth. The porphyry contains 5 percent rounded quartz, and 20 to 30 percent plagioclase as phenocrysts 1 to 2 cm long. Approximately 5 percent biotite occurs as irregular clots and subhedral books 1 mm across. The phenocrysts are set in an aplitic groundmass consisting of equant grains of quartz and K-feldspar 0.1 mm in diameter; these have a mosaic texture in thin section, and the ratio of quartz to K-feldspar is approximately 2 : 3.

Late, narrow dikes of quartz latite porphyry occur along the western contact of the stock. Although their mineralogy is somewhat variable and they may represent more than one magmatic surge, their phenocryst content may be characterized as follows: 10 to 25 percent plagioclase, 5 percent rounded quartz, 5 percent biotite, and sparse K-feldspar. The sizes of phenocrysts are comparable to those in the quartz monzonite porphyry, with the exception of quartz phenocrysts, which attain a diameter of 2 to 5 mm. Specimens with high phenocryst content closely resemble the quartz monzonite porphyry. The groundmass is usually medium to dark brown due to abundant fine biotite grains.

Alteration and mineralization: Alteration and mineralization of the western portion of the Bingham stock near the present surface consists of secondary biotite + orthoclase accompanied by chalcopyrite + pyrite. A weakly developed sericitic overprint is present in a northeast-trending zone near the western contact; elsewhere, biotite-orthoclase alteration grades outward to propylitic alteration. Details of these patterns are presented in other papers of this issue (Moore; Lanier et al.; John).

The igneous rocks at depth north of the Apex shaft are only weakly mineralized. Quartz monzonite and quartz monzonite porphyry contain some disseminated chalcopyrite and average about 0.1 to 0.2 percent copper adjacent to the high-grade skarns in the major limestone beds at elevations between 1,500 and 1,200 m. Below 1,200-m elevation, the porphyry is nearly barren of copper, averaging approximately 0.01 to 0.05 percent copper. Thus, the intrusive system at the deeper levels of the high-grade skarn zone probably corresponds to the molybdenite zone and barren core zone of James (1971) and John (1975).

Both quartz monzonite and porphyry contain an alteration assemblage characteristic of the potassium silicate zone as defined by Meyer and Hemley (1967). Biotization of hornblende and augite (Bray, 1969; Moore and Czamanske, 1973; Lanier et al., 1975)

TABLE 1. Two Typical Sequences of Calc-Silicate Zoning in Thin Limestone Beds

Spatial relation	Calc-silicate assemblage	Rock type
overlying siltstone	quartz-tremolite-diopside	silty hornfels
upper contact of ls bed	calcite-tremolite	pale green silicated marble
transitional zone	calcite-talc	white marble
central portion of ls bed	calcite-dolomite	black dolomitic limestone
overlying siltstone	quartz-calcite-tremolite-diopside	silty hornfels
upper contact of ls bed	talc-tremolite	white to pale green silicated marble
transitional zone	calcite-talc-tremolite	white to pale green silicated marble
central portion of ls bed	calcite-talc	black limestone

is pervasive, and locally the plagioclase phenocrysts in porphyry are partially replaced by veinlets of fine-grained, sugary K-feldspar. In some specimens the texture of the porphyry is almost obliterated, and the magmatic biotite is largely replaced by K-feldspar. Rutile is commonly disseminated in areas of K-feldspar replacement, apparently a product of biotite destruction.

In addition to the typical products of potassium silicate alteration, plagioclase throughout most of the igneous rocks drilled is partially to completely replaced by a fine-grained, pale blue mixture of montmorillonite and sericite. Only plagioclase was affected; K-feldspar and biotite apparently remained stable. Moore and Nash (1974) described similar pervasive alteration of plagioclase to sericite, kaolinite, and minor amounts of montmorillonite in porphyry on the western edge of the stock above the present pit surface. Kaolinite is not present in samples X-rayed by us, and montmorillonite occurs in major concentrations. Possibly the rocks studied by Moore and Nash had been affected by acid mine water which converted the montmorillonite largely to kaolinite.

Early Contact Metasomatism

The Early Stage of contact metasomatism resulted in the pervasive development of interstitial diopside in quartzite, diopside-quartz hornfels in interbedded calcareous siltstone, and wollastonite with minor diopside, idocrase, and garnet in thick units of cherty limestone. Minor sulfide deposition may have accompanied silication of siltstone and cherty limestone during this Early Stage, although unambiguous evidence is lacking.

Mg metasomatism in quartzite and thin interbedded limestone

The extensive supergene leaching and clay alteration of surface exposures has destroyed much of the original mineralogy. Because of this, and also because of lack of exposures in critical areas, the following descriptions are based largely on the study of samples and thin sections from drill cores.

Contact metasomatic calc-silicates are recognized up to 1,500 m from the northwestern contact of the Bingham stock. Metasomatic dolomite extends an unknown distance beyond this limit. The outer edge of silication is controlled in detail by lithology and structure; it extends farthest from the stock in quartzite and along major fault zones. The zonal pattern of the Early Stage in quartz-rich rocks consists of a diopside zone near the intrusive, and an outer transition zone.

Outer transition zone: The mineralogy of the outer transition zone generally is not a mappable feature, other than the gradual disappearance of interstitial calcite as the stock is approached.

In rocks with abundant quartz, which originally were calcareous quartzite, the transition zone averages 240 m in width [1] and is characterized by three-phase assemblages. Talc is the first silicate to appear, at 1,500 m from the stock. Calcite and quartz are ubiquitous, and the third phase changes systematically from talc to tremolite and finally to diopside with increasing proximity to the stock. The inner half of the transition zone is characterized by diffuse amoeboid patches containing the assemblages quartz-calcite-diopside or quartz-tremolite-diopside; the surrounding quartzite contains the assemblage quartz-calcite-tremolite or, more rarely, quartz-calcite-tremolite-diopside. Calcite and tremolite generally disappear at the same point, some 1,200 m from the stock; this point marks the outer boundary of the diopside zone.

Black dolomitized limestone beds, 1 to 3 m thick and interbedded with quartzite and calcareous siltstone, commonly survive without bleaching or silication to within 1,200 m of the intrusive contact. Diopside appears at the upper and lower contacts of these thin beds, and the transition to the central unsilicated portion of the bed is measured generally in centimeters; some typical zonal sequences are summarized in Table 1. Within 600 m of the stock, all thin limestone beds are pervasively silicated and consist of diopside or diopside-quartz.

[1] All distances and widths are measured at right angles to the intrusive contact, which dips 60° NW.

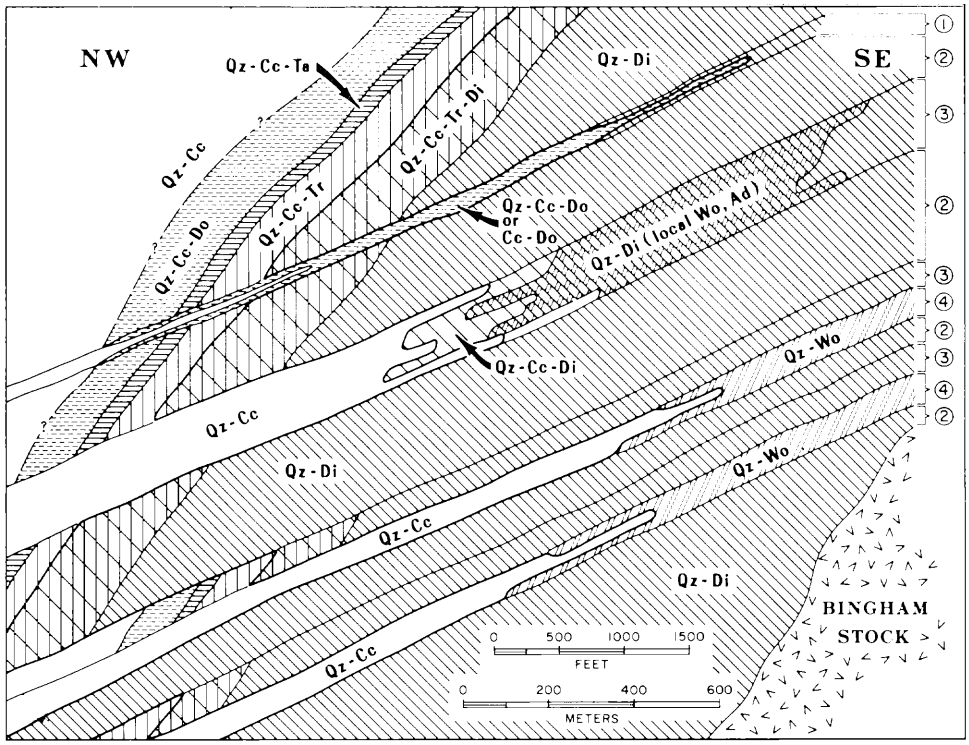

FIG. 4. Schematic cross section looking northeast along the intrusive contact north of the Bingham syncline illustrating Early Stage alteration zoning. Heavy line represents the outer limit of diopside. Original lithology: (1) thin limestone; (2) quartzite and calcareous quartzite; (3) interbedded calcareous siltstone, silty limestone, limestone (e.g., Tilden series); (4) thick cherty limestone (e.g., Yampa limestone member). Abbreviations as in Table 2.

The transition zone as described above has been noted in core from several of the westernmost drill holes located northeast of the Apex shaft. However, on the surface, an exposure of the Tilden series east of the Apex shaft indicates that the transition zones may not always be present. Here, diopside-quartz hornfelses pass directly into apparently unaltered calcareous siltstones. In thin section, diopside can be seen to have replaced calcite directly with no intervening tremolite, talc, or dolomite. This relation suggests that there was a marked variation in the T-X_{CO_2} conditions which prevailed at any given point at the Mg-metasomatic front.

Diopside zone: The average width of the diopside zone is 1,200 m in quartzite and 900 m in calcareous siltstone. Prior to the Main Stage, this zone contained an average of 30 to 35 percent diopside; diopside is the most abundant metasomatic mineral in the contact aureole. Its local abundance within individual stratigraphic units is clearly dependent on the original calcite content of the rock, a fact which has allowed the mapping of stratigraphy within the altered zone. Sedimentary features such as cross-bedding and quartz grain size and distribution are preserved in detail. The freshest diopside is white to pale blue green but weathers readily to a characteristic buff color. Locally, diopside occurs in gash veinlets, but the overwhelming majority occurs interstitial to quartz grains and forms intergrowths of equant grains a few microns in diameter. Adjacent quartz shows only minor embayment. Calcite is absent.

Within the originally more calcareous portions of the formation, such as the Tilden or IXL series, certain beds in the outer portion of the diopside zone locally contain the assemblages quartz-wollastonite-diopside and quartz-wollastonite. Garnet, close to andradite in composition, occurs sparingly in irregular patches closely associated with wollastonite-bearing rocks. Within 300 m of the stock, both wollastonite and garnet disappear, and the diopside zone consists exclusively of quartz-diopside.

Sulfide: Evidence for sulfide deposition during the Early Stage in quartzite and interbedded thin silty limestone is generally lacking or ambiguous. Much of the pyrite and chalcopyrite present in the rock is clearly related to the Main Stage, which overlapped the diopside zone to within 30 to 50 m of the outer transition zone. Pyrite, sphalerite, and galena are present in very minor amounts in the transition zone, in some cases occurring on Late

fractures coated with clay and also as disseminations in apparent equilibrium with diopside-calcite-quartz.

Two types of occurrences suggest that some sulfide deposition was contemporaneous with the Early Stage of silication: (1) Andradite spots in quartz-wollastonite-diopside hornfels of the Tilden and IXL series are generally accompanied by minor disseminations of chalcopyrite and galena with traces of sphalerite. Wollastonite-bearing rock in the Tilden and IXL series generally contains disseminated galena, some sphalerite, and traces of chalcopyrite even where andradite is absent. (2) The transition from calcite-talc marble to calcite-tremolite skarn in thin silty limestones generally is the site of massive streaks a few centimeters thick of pyrite, magnetite, and traces of chalcopyrite.

Interpretation: A reconstruction of the distribution of silicate assemblages in the contact aureole is presented schematically in cross section in Figure 4. Three major differences are apparent in contrasting the quartzite zonal pattern with that of the interbedded thin silty limestones:

1. The limestone assemblages quartz-calcite-dolomite, calcite-talc, and calcite-tremolite occur well within 1,200 m of the stock in areas where adjacent quartzite is pervasively altered to quartz-diopside.

2. The transition zone separating quartz-calcite-dolomite from diopside or quartz-diopside in thin limestone beds occurs over a few centimeters to one meter, whereas the same transition in quartzite occurs over 250 m.

3. Some of the more consistently highly calcareous series of beds, such as the Tilden, lack the transition through dolomite, talc, or tremolite-bearing assemblages and pass directly from quartz-calcite to quartz-calcite-diopside. These are the beds which develop wollastonite in the outer portion of the diopside zone.

The above relationships indicate the important influence of permeability on the zonal pattern. Apparently, the higher the original quartz content, the higher the effective permeability. Enhancement of permeability was due largely to the different responses of the beds to Cretaceous deformation; the quartzites fractured whereas the more limy beds deformed to some degree by flowage and hence retained their cohesiveness. Mg-bearing fluids infiltrated the quartzites to some distance from the stock but did not gain access to the interbedded, thin silty limestones except where these were thin and enclosed in quartzite sections.

Amphiboles and pyroxenes in the transition zone are typically white to pale green and hence are presumed to contain very little iron. Pyroxene from a typical quartz-diopside hornfels contains 4 mole

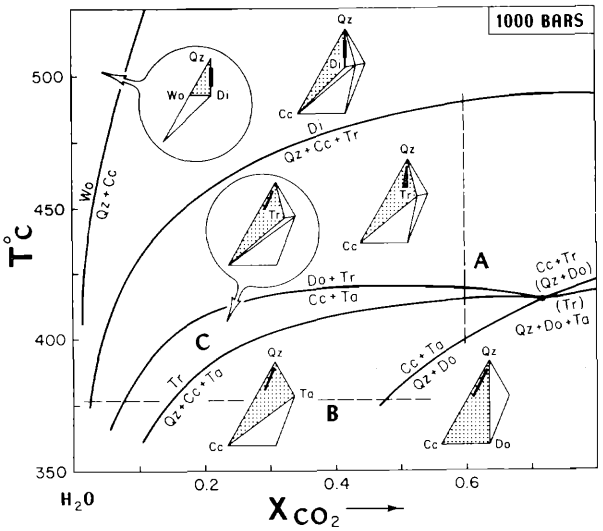

FIG. 5. Partial T-X_{CO_2} diagram at 1,000 bars total pressure for the system CaO-MgO-SiO_2-CO_2-H_2O, from Slaughter et al. (1975). Stippled three-phase triangles represent assemblages noted in quartzite and calcareous quartzite whose bulk composition, estimated from mineral proportions, is represented by the black bars. Dashed line gradients A and B are discussed in text. Abbreviations as in Table 2.

percent hedenbergite (Table 6, no. 1). As a first approximation therefore, mineral stabilities may be discussed in terms of Mg end members. The latest version of the T-X_{CO_2} diagram for the system CaO-MgO-SiO_2-CO_2-H_2O at 1,000 bars total pressure (Slaughter et al., 1975) is presented in Figure 5. The sequence of mineral assemblages in the transition zone could be the result of a thermal gradient at constant values of X_{CO_2} around 0.6 (path A, Fig. 5); for such a path, the minimum thermal gradient would be from 390° to 485°C over the 240-m width of the transition zone. The zonal pattern could also result from an isothermal gradient in X_{CO_2} below 400°C (path B, Fig. 5). In such a case, fluids on the fringe of the pattern would be relatively higher in X_{CO_2} than those in the interior. The data on assemblages alone cannot resolve the choice between these two paths or intermediate paths. They do, however, restrict the fluid compositions to the water-rich side of the invariant point quartz-calcite-dolomite-talc-tremolite (Fig. 5). The one field relation which is compelling evidence for the local existence of CO_2 gradients as an important control of phase assemblages is the existence of intimately interstratified quartz-diopside beds and calcite-talc beds separated in some cases by only a few centimeters of intermediate assemblages. It is much more likely that fluid composition gradients existed between adjacent beds than temperature gradients.

Figure 5 summarizes the phase equilibria in calcareous quartzite in which quartz remained in excess

throughout and the only effect of Mg-metasomatism was to progressively lower the ratio of calcite to dolomite, talc, tremolite, or diopside. Metasomatism of a rock whose bulk composition fell near the quartz end of the quartz-calcite tie line yielded a rock approximately on the quartz-diopside tie line. The T-X_{CO_2} conditions at which Mg metasomatism began at any given point in the aureole determined which Mg phase appeared first. The phase sequence was insensitive to minor variations in percent SiO_2 imposed by local differences in detrital quartz content.

In silty limestone, Mg metasomatism also began on the quartz-calcite tie line but, in contrast with the quartzite, the abundance of calcite led to several different possible assemblages for any given T-X_{CO_2} facies. For example, in the case of the facies labeled C (Fig. 5), a SiO_2-poor bed with the same Ca/Mg ratio as interbedded quartzite could yield the following assemblages, dependent on slight differences in original quartz content: calcite-tremolite, calcite-talc, or calcite-dolomite. Because the zoning in these thin horizons is parallel to bedding, it is virtually impossible to distinguish between the effects of metasomatism and the effects of variations in original quartz content.

Mg metasomatism of silty limestone either terminated on the quartz-diopside tie line or resulted in monomineralic diopside hornfels; it is clear that a substantial amount of silica had to be added in addition to magnesium.

Although the quartzite zonal pattern can be treated in terms of a relatively unambiguous T-X_{CO_2} model, the zonal patterns in interbedded silty limestone are complex and do not yield to a simple explanation. The presence of the assemblage calcite-talc, indicative of temperatures less than 415°C and X_{CO_2} less than 0.7 at 1 kb total pressure, in close association with quartz-diopside, indicative of relatively higher temperatures and/or lower X_{CO_2}, does place some constraints on the T-X_{CO_2} path in both lithologies. The vast majority of the aureole's sedimentary rocks were permeable to Mg-bearing fluids at T-X_{CO_2} conditions outside the wollastonite stability field. The resulting zonal pattern consists of Mg-rich hydrous calc-silicates replaced on the intrusive side by the anhydrous phases diopside or diopside-wollastonite. This is in sharp contrast to the pattern in the thick cherty limestone members of the lower part of the Bingham Mine Formation which were not permeable to metasomatic fluids until after they largely had been converted to wollastonite.

Wollastonite zone in limestone

The skarn zonal pattern in the Highland Boy and Yampa limestones may be described in terms of two zones, each of which shows some variation in mineralogy and proportions of phases: an outer wollastonite zone and an inner garnet zone. These two zones locally can be interpreted as contemporaneous products of zoned skarn formation; however, the districtwide distribution of wollastonite suggests that in part it may be early and unrelated to the development of the garnet zone.

The wollastonite zone contains the primary minerals wollastonite, diopside, calcite, quartz, and accessory idocrase, andradite and sulfides. Contrary to Stringham's (1953) assumption that the limestone beds were originally dolomitic, Lindgren's (1924) chemical data and the mineralogy of the outer silication zone clearly indicate that the limestone beds contained insignificant magnesium. As the stock is approached, chert nodules in black limestone are bleached and surrounded by a rim of wollastonite. As silication increases, chert nodules and chert layers are almost completely replaced by wollastonite, and interlayers of limestone are bleached and recrystallized. Closer to the stock, these thin, bedding-controlled lenses of white marble contain as much as 20 percent wollastonite as disseminated clots of radiating fibrous crystals. Interbedded layers of fine-grained, sandy to flinty white hornfels containing wollastonite-quartz or wollastonite-diopside-quartz presumably represent chert lenses. Brown idocrase, identified by X-ray and in thin section, is a minor but characteristic phase of the wollastonite zone. Its distribution is not known in detail, but it occurs with andradite and diopside. Small amounts of disseminated chalcopyrite, bornite, sphalerite, and galena are most commonly associated with andradite spots and veins and are presumed to be stable and contemporaneous with Early garnet.

The wollastonite zone separates the Main Stage garnet zone from limestone or marble. At the surface and in the upper mine levels, the wollastonite zone first appears beyond garnet, generally in the central portions of the beds, and extends as a pervasive replacement of the beds an additional 150 to 180 m. Beyond this limit, the wollastonite zone fingers out along bedding, largely at the footwall or hanging wall of the beds, and extends to an outer limit of silication some 600 m from the porphyry. At depth in the northern limb of the Apex fold, below 4,300 ft elevation, the wollastonite zone is considerably more restricted in extent and locally the garnet zone is in direct contact with limestone.

The garnet zone is absent or only locally developed in limestone on the eastern and southern contacts of the Bingham stock. Pervasively garnetized limestone xenoliths are found in the quartz monzonite phase of the stock and generally within 450 m of the porphyry contact. Limestone along the southern

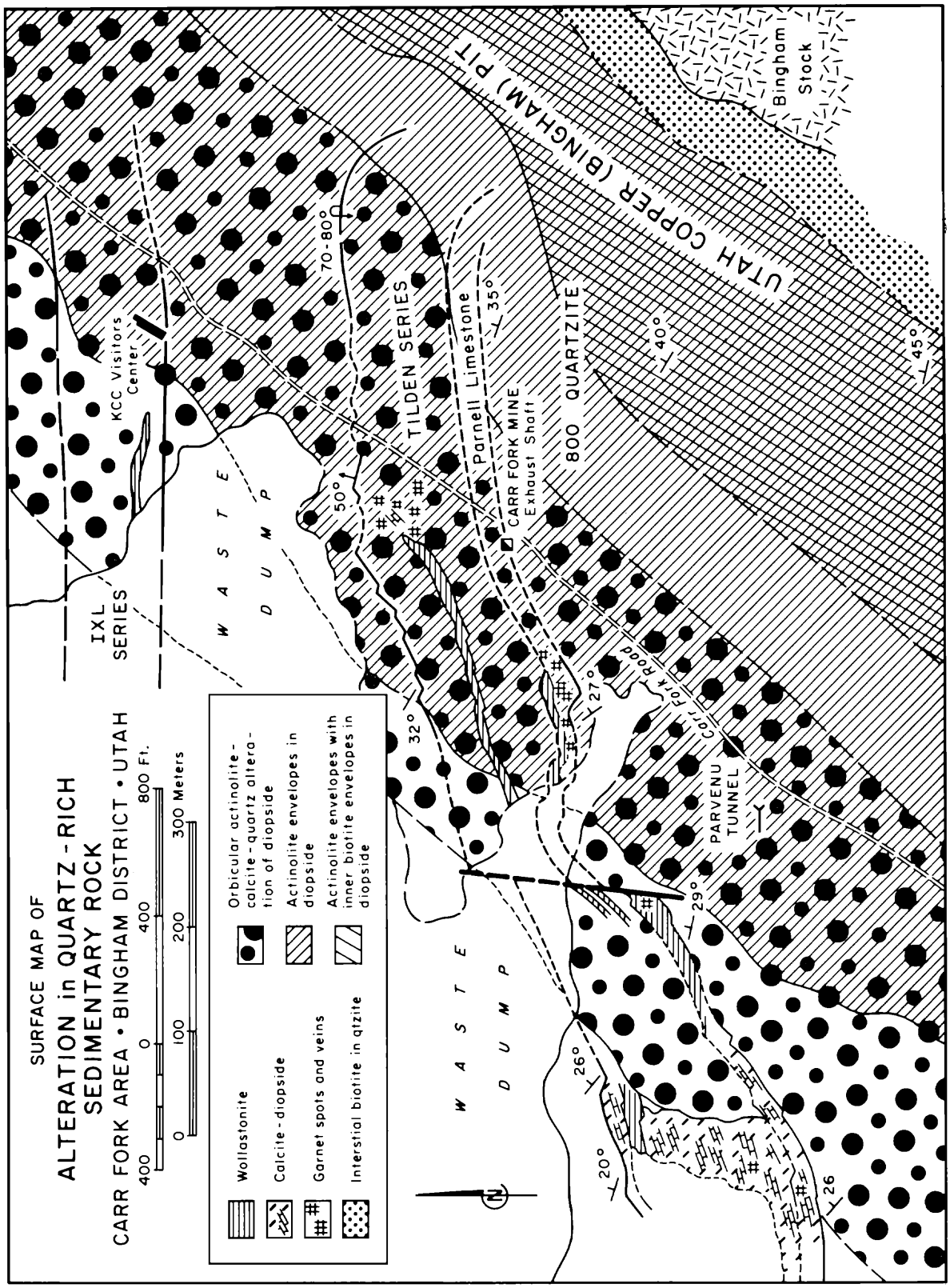

FIG. 6. Alteration in quartz-rich sedimentary rock mapped in surface exposures, Carr Fork area.

contact of the Bingham quartz monzonite largely is converted to wollastonite, and here the wollastonite zone is continuous to the northern contact of the Last Chance quartz monzonite in the U. S. mine, a distance of 1,500 m from the porphyry. In the Lark mine, silication, silification, and bleaching extend approximately 650 m from the quartz monzonite (Rubright and Hart, 1968), and garnet is present locally within 100 m of the contact (Rubright, pers. commun., 1976).

Available information on the character and extent of silication in limestone near the Last Chance stock suggests that it is less extensive than that associated with the Bingham stock and that the garnet zone is absent. In the Utah Metals mine, black limestone is present locally within 30 m of the contact, and the silication is typical of the wollastonite zone. On the eastern contact of the Last Chance stock in the U. S. mine, limestone is pervasively silicated in a zone 75 m wide and contains wollastonite and diopside with minor idocrase and garnet (Field and Moore, 1971).

The above facts lead to the following general conclusions:

1. The wollastonite zone is most extensive within the wall-rock septum between the equigranular quartz monzonite of the Bingham and Last Chance stocks. This relation suggests that the wollastonite zone in this area formed, at least in part, at the time of emplacement of quartz monzonite.

2. The garnet zone is symmetrical about the quartz monzonite porphyry and is absent along the majority of equigranular quartz monzonite contacts located 450 m or more from the porphyry contact. district scale, generally may be late relative to the Garnet, in contrast with wollastonite, is clearly related to the emplacement of the porphyry and, on a wollastonite zone. Near the surface in the western contact zone, however, wollastonite may have continued to form in marble as the Main Stage garnet zone advanced from the porphyry side. At depth, the garnet zone locally bypassed the wollastonite zone and encroached directly onto limestone. An increase in P_{fluid} and/or an increase in X_{CO_2} with depth could have inhibited the formation of wollastonite.

Main Stage Alteration and Mineralization in Quartzite and Thin Silty Limestone

Quartz-sulfide veinlets with biotite and actinolite alteration envelopes in diopside-bearing quartzite and interbedded diopside-quartz hornfels represent the Main Stage of alteration and mineralization. Vein relations at contacts with the stock indicate that this stage was contemporaneous with quartz-sulfide veining and biotite-orthoclase alteration of igneous rocks. Mineralogical zoning of the Main Stage in quartz-rich rocks is summarized in Figures 6, 7, and 8, and Table 2.

Actinolite

Actinolite replaced diopside in the outermost zone of alteration related to sulfide deposition. In silty diopside hornfels, actinolite largely is restricted to envelopes on quartz-sulfide veinlets and patches and extends from the intrusive contact outward to within a short distance of the outer edge of the diopside zone (Figs. 6, 7A, and 7B). In diopsidic quartzite, actinolite completely replaced diopside in a zone 150 m wide next to the stock and is restricted to veinlet margins farther out. Actinolite alteration does not extend beyond the outer edge of the Early diopside zone.

TABLE 2. Summary of Mineral Assemblages in Quartzite and Thin Silty Limestone, Listed in Order from Outer Zones to Intrusive Contact

	Quartzite and interbedded silty limestone	Limestone in Tilden series
Early Stage		
	Qz-Cc	Qz-Cc
	Qz-Cc-Do	Qz-Cc
	Qz-Cc-Ta	Qz-Cc
	Qz-Cc-Tr	Qz-Cc
	Qz-Cc-Tr-Di	Qz-Cc
	Qz-Cc-Di	Qz-Wo-Di-Ad
	Qz-Di	Qz-Wo-Di-Ad
Main Stage		
	(Di)Qz-Ac (orbicules and envelopes)	(Di)Qz-Ac (orbicules and envelopes)
	(Di)Qz-Ac-Bio (envelopes)	(Di)Qz-Ac (envelopes)
	Qz-Bio (envelopes), Qz-Ac (pervasive)	(Di)Qz-Ac, Qz-Bio (envelopes)
	Qz-Bio (pervasive)	(Di)Qz-Ac, Qz-Bio (envelopes)
	Qz-Bio-Or	(Di)Qz-Bio (envelopes), Qz-Ac (locally pervasive)
	Intrusive	Intrusive

Abbreviations: Qz = quartz, Cc = calcite, Do = dolomite, Ta = talc, Tr = tremolite, Wo = wollastonite, Di = diopside, Ad = andradite, Ac = actinolite, Bio = biotite, Or = orthoclase, (Di) signifies unaltered diopside relicts from Early Stage.

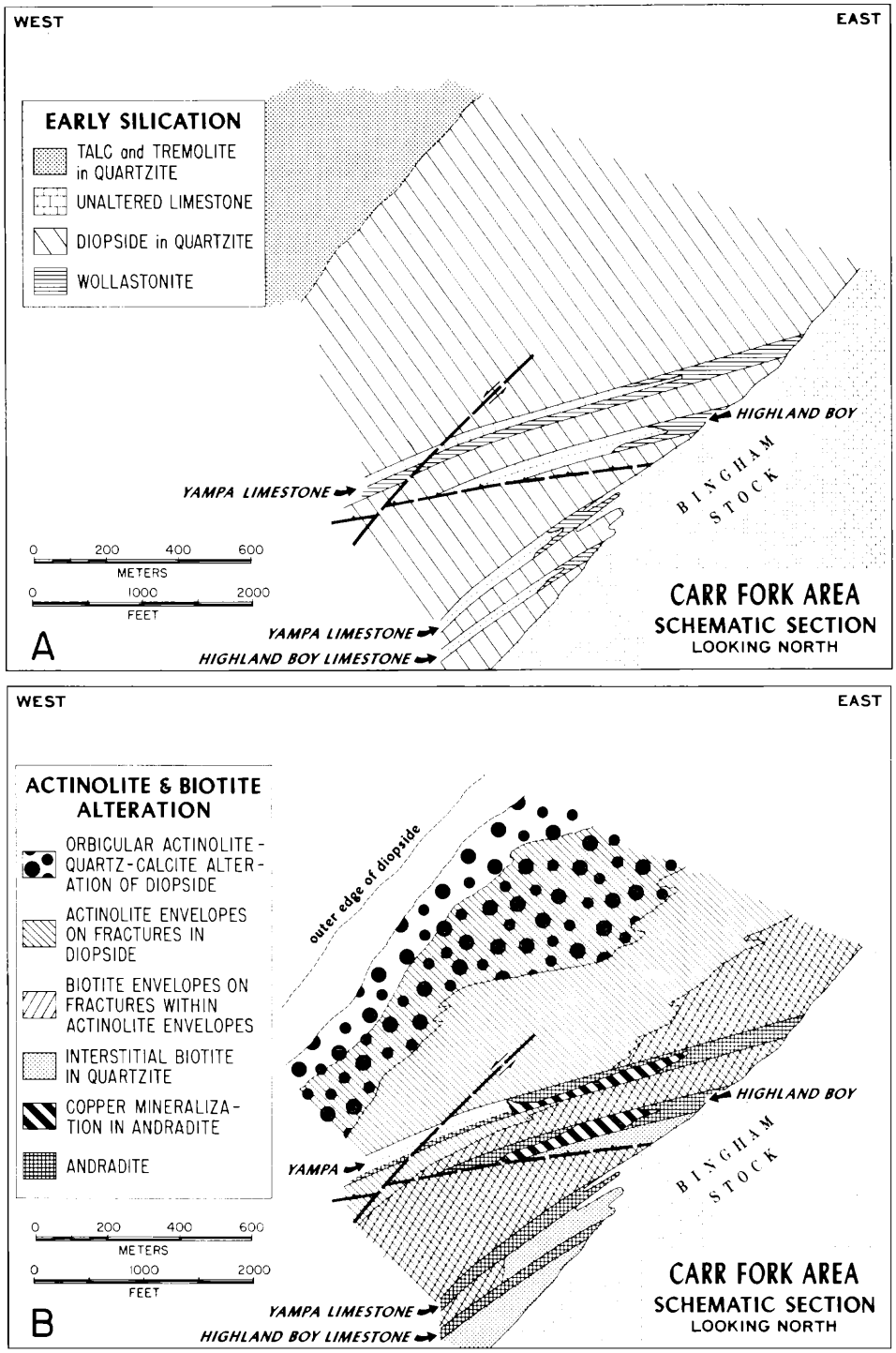

FIG. 7. Vertical east-west cross sections, based on data from drill holes spaced approximately 300 m apart, illustrating zonal patterns of alteration in sedimentary rocks.

A. Early magnesium metasomatism and silication patterns, illustrating extent of diopside in quartzite and of wollastonite in limestone.

B. Main Stage alteration pattern, illustrating extent of actinolite and biotite in diopsidic quartzite and of garnet and high-grade copper mineralization in limestone.

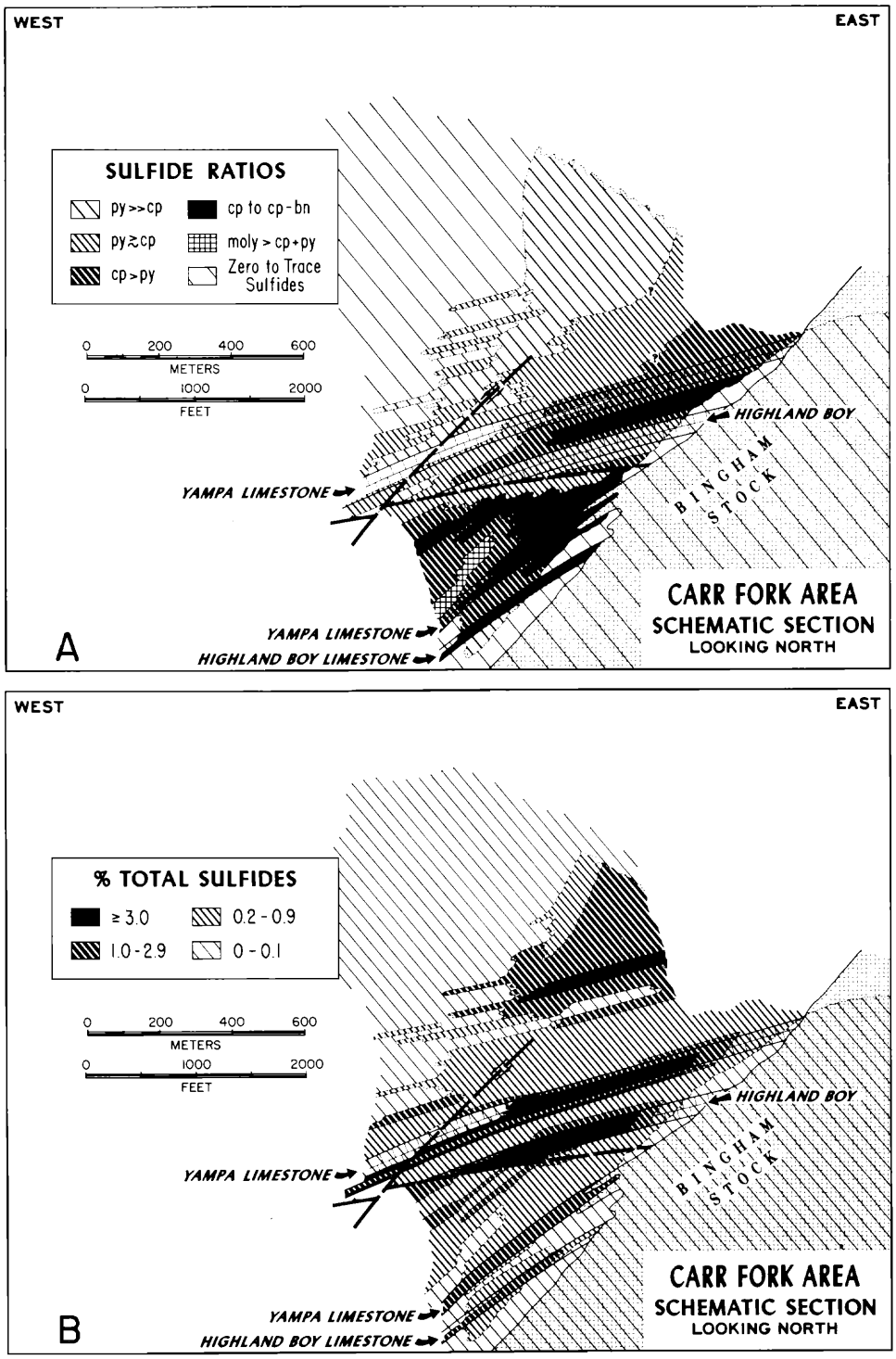

FIG. 8. Vertical east-west cross sections, as in Figure 7, illustrating sulfide distribution patterns.

A. Zoning of sulfide ratios, based on visual estimates. Chalcopyrite is essentially restricted to the actinolite envelope zone and biotite zone; the zones of dominant chalcopyrite (cp > py, and cp) roughly coincide with biotite alteration.

B. Zoning of total sulfide abundance, based on visual estimates, showing strong dependency on lithology and distance from intrusion. Highest sulfide content occurs in zones of biotite-actinolite and garnet.

Actinolite alteration of diopside exhibits three textural variants: bedding streaks, orbicules, and envelopes on fractures. These variants are zoned relative to the intrusive contact, with bedding streaks occupying an outermost zone and envelopes occupying an innermost zone.

Bedding streaks: In the outermost zone, actinolite occurs in white diopside as light to medium green, irregular streaks along bedding. The thickness of individual streaks varies from a centimeter to a few tens of centimeters, but the lateral dimensions are unknown because bedding streaks have been noted only in drill core. Disseminated pyrite often is associated with the actinolite, and some occurrences exhibit an outer silicified shell a few millimeters thick. Closer to the stock, silicified areas occur at the center of actinolite streaks; this represents a gradation to the next textural variant, orbicular aleration.

Orbicular texture: Orbicular alteration is characteristic of the next zone inward, which is 200 to 500 m thick (Figs. 6 and 7B). The orbicules typically are ovoid in shape, generally 0.5 to 15 cm in diameter, but average about 2.5 cm. The largest occur in quartzite, and one exceptional example 30 cm in diameter was found. The orbicules consist of quartz and actinolite, locally containing calcite and sulfides. The arrangement of the minerals consists of an outer layer, generally 1 to 3 mm thick, of finely fibrous actinolite (0.01 × 1 mm) around a quartz core (Fig. 9A and B), which commonly contains a clot of coarsely fibrous actinolite at the center. Less commonly, multiple shells of actinolite plus quartz are separated by monomineralic quartz shells; in one such example, six cycles of actinolite-quartz are present. In hornfels, the inner and outer boundaries of the actinolite shell are sharply defined, whereas in quartzite they are more diffuse. In some areas, calcite with or without actinolite occurs as clots in the quartz core, and calcite is sometimes present in the outer actinolite layer. The calcite-actinolite assemblage occurs in the outer 200 m of the orbicular zone. Closer to the intrusion, this assemblage was not noted in orbicules. Rarely the orbicules occur in areas of garnet-bearing diopside hornfels. Here garnet was found at the centers of silicified orbicules, associated with calcite and actinolite. In many cases sulfides are present at the center or within the quartz-rich portion. The sulfides are usually pyrite, but chalcopyrite, galena, and sphalerite are present in some locations.

The argument has often been advanced in informal field discussions that some of the orbicules represent original chert nodules in the sedimentary rocks. If we were to assume that the orbicules reflect replaced chert nodules, chert abundance must have been two orders of magnitude greater than that now visible in the stratigraphically equivalent unaltered rocks. In fact, chert is absent from most of the quartzite, and it is rare in the thin interbedded limestone beds. The most convincing evidence that these are not chert nodules is that in quartzite the orbicules are mostly aligned along fractures that cut bedding

TABLE 3. Chemical Analyses of Amphiboles

	1	2	3
SiO_2	54.76	54.20	49.06
TiO_2	0.00	0.21	0.83
Al_2O_3	0.42	0.62	6.28
Fe_2O_3	1.78	5.67	4.11
FeO	1.20	6.94	4.56
MnO	0.04	0.14	0.10
MgO	23.30	16.91	17.67
CaO	13.29	12.76	12.88
Na_2O	0.32	0.37	1.01
K_2O	0.19	0.20	0.51
P_2O_5	0.00	0.00	0.00
F^-	0.95	0.38	0.50
S	0.07	0.04	0.04
$+H_2O$	1.16	1.25	1.84
Total	97.48	99.69	99.39
−O Correction for F^-	0.40	0.16	0.21
−O Correction for S	0.04	0.02	0.02
Total	97.04	99.51	99.16

Number of cations on basis of 24 oxygens, hydroxyls, and fluorines

	1		2		3	
Si	7.82		7.83		7.04	
Ti	0.00	7.89	0.02	7.96	0.09	8.19
Al	0.07		0.11		1.06	
Fe^{+3}	0.19		0.62		0.44	
Fe^{+2}	0.13		0.83		0.54	
Mn	0.01	5.29	0.02	5.11	0.01	4.77
Mg	4.96		3.64		3.78	
Ca	2.03		1.97		1.98	
Na	0.09	2.15	0.10	2.11	0.28	2.35
K	0.03		0.04		0.09	
F	0.43	1.54	0.17	1.37	0.02	1.78
H	1.11		1.20		1.76	
Total	16.87		16.55		17.09	
Fe/Fe + Mg	0.06		0.28		0.21	

Analyses by James Cardwell. Wet analytical methods.

1. White coarsely fibrous tremolite, from a late Main Stage or early Late Stage fracture, cutting massive light green actinolite at the top of the garnetized Highland Boy limestone, 100 m from porphyry.

2. Light green actinolite, from actinolite alteration of a diopside hornfels bed in the quartzite sequence, 15 m above the Yampa limestone. Associated with diopside, quartz, chalcopyrite, pyrite, and magnetite. From the outer part of the biotite zone, 200 m from porphyry.

3. Dark green actinolite, from massive actinolite skarn with locally abundant green and brown micas and a trace of chalcopyrite. Believed to be endoskarn, associated with recognizable igneous rocks at the contact between Highland Boy limestone and the Bingham stock.

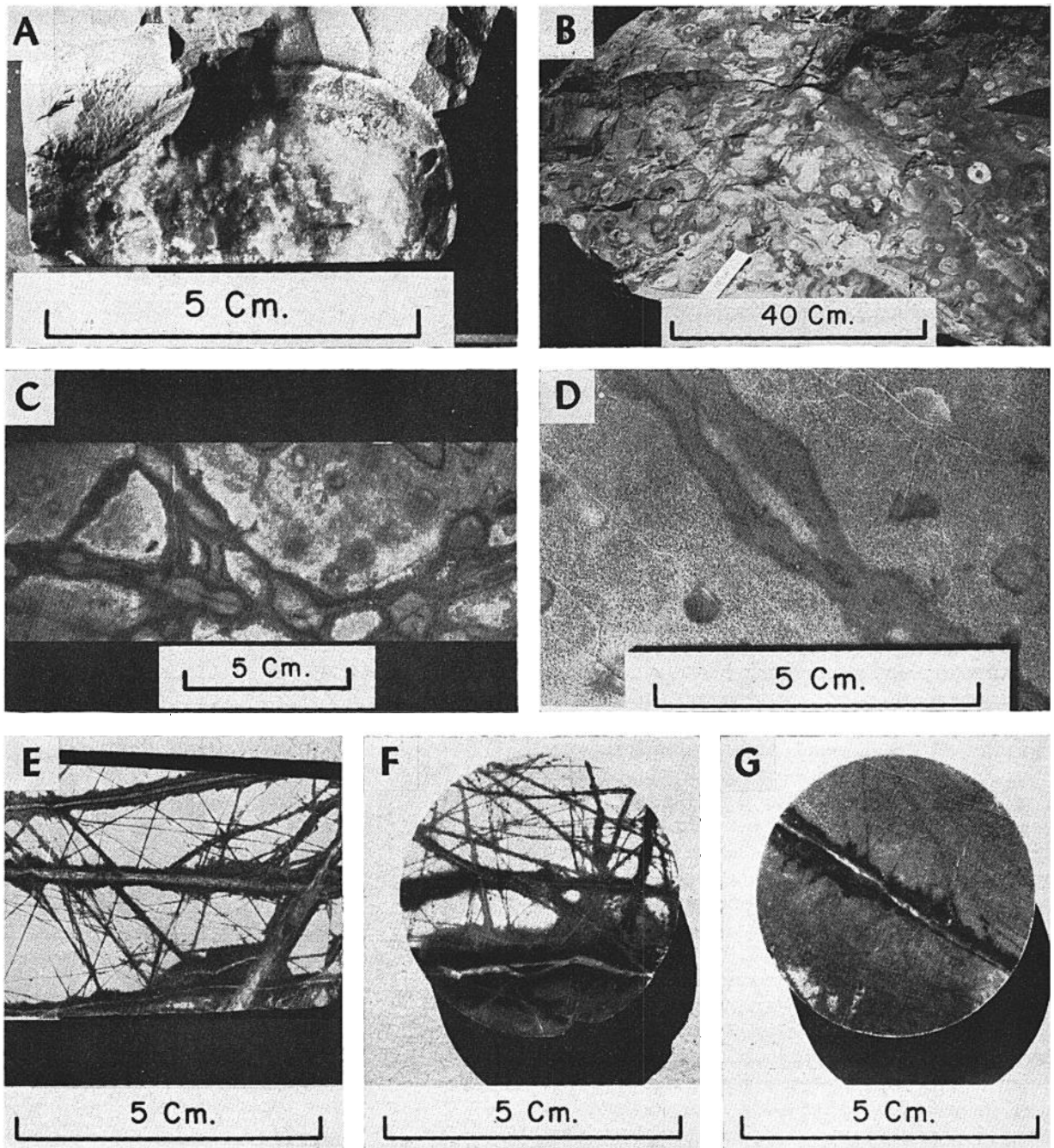

FIG. 9. A. Orbicular alteration in diopside hornfels. Rim is fine-grained actinolite, core is quartz containing some coarse-grained calcite, fibrous actinolite, and pyrite. Apparent layering of rim is due to supergene effects.

B. Orbicular alteration in diopside hornfels, in outcrop, showing density of orbicules. Some fracture-controlled envelopes are also apparent.

C. Orbicular alteration in diopside-rich quartzite, showing orbicules aligned on fractures. Actinolite rims on orbicules are limonite stained.

D. Fracture-controlled alteration envelope in orbicule zone of diopside-rich quartzite. Detrital quartz grains are dark, hydrothermal quartz and calc-silicates are light.

E. Densely spaced actinolite envelopes along fractures in diopside hornfels. Vein fillings are quartz-calcite with trace molybdenite. Near-horizontal vein at top of specimen has a thin inner biotite envelope.

F. Quartz-calcite vein with strong biotite envelope and outer actinolite envelope in diopside-rich quartzite. Typical of actinolite-biotite zone.

G. Quartz-calcite vein with biotite envelope in an area of coalesced actinolite envelopes. Small remnant of diopside visible at lower left. Typical of innermost biotite-actinolite zone.

(Fig. 9C), and this relation occurs commonly in hornfels as well. Locally in quartzite the alteration has been so extensive that the orbicules have coalesced, resulting in patchy remnants of diopside and actinolite.

Contact aureoles in many districts commonly show spotted textures where nucleation of a mineral has been restricted. At Carr Fork, the orbicules represent a special variety of such textures, and their origin may be interpreted as follows: Diffusion in an intergranular pore fluid fed from nearby fractures was responsible for transfer of materials to and from sites of nucleation. The solution presumably was in a metastable state between nucleation sites where it was supersaturated with respect to quartz, actinolite, and sulfides. Closer to the intrusion, orbicules are absent and alteration envelopes formed uniformly along the fractures, without apparent delays in nucleation or supersaturation. The envelope type of alteration expanded outward with time into the inner part of the orbicular zone. Thus, solutions traveling outward from the intrusion passed from a zone characterized by local equilibrium with the walls of fractures outward into a zone where conditions were metastable between orbicules. With time, the zone of envelopes expanded outward until this stage of alteration terminated.

The geometrical and age relations of the orbicule and envelope zones may have been due to thermal gradients adjacent to the Bingham stock. The inner boundary of the orbicule zone may represent the isotherm of a critical temperature below which equilibrium was no longer maintained and solutions became supersaturated.

Envelope textures: A complete gradation exists from orbicules along fractures to orbicules which have partly coalesced, to fracture envelopes with wavy margins (Fig. 9C and D), to those with margins which are parallel to sulfide-bearing fractures (Fig. 9E). In the transition from the orbicule zone to the envelope zone, alteration envelopes on calcite-bearing fractures commonly have the same mineralogy as the orbicules: inner envelopes of quartz and outer envelopes of actinolite. Within 200 to 150 m of the intrusive contact, the inner quartz envelopes disappear and the alteration consists of actinolite with or without calcite and quartz. In this inner zone, the density of fractures is greater than farther out (compare Fig. 9D and E).

One analysis of actinolite from the envelope environment indicates 28.6 mole percent ferrotremolite end member (Table 3, no. 2). This amphibole is light green in color, no darker than that in the orbicular alteration. Toward the intrusion the color of amphiboles becomes much darker and presumably richer in iron.

Biotite

About 450 m from the intrusion, a few rare fractures contain an inner envelope of dark brown biotite and an outer envelope of actinolite (Fig. 9F and G). Such inner biotite envelopes become more common in quartzite toward the stock to a point where they coalesce and, within 50 m of the stock, actinolite is no longer present (Fig. 7B). In diopside hornfels, in contrast, inner biotite envelopes are rare near the stock. More commonly, quartz-chalcopyrite veinlets which cut the contact between biotized igneous rock and diopside hornfels contain biotite envelopes in igneous rock and actinolite envelopes in hornfels. These veinlets suggest a close genetic relationship between biotite-orthoclase alteration of the stock and actinolite alteration of diopside in quartz-rich sedimentary rocks.

Many biotite-bearing envelopes contain chalcopyrite and some contain bornite. Biotite in this association is always a dark brown. However, the most common vein mineralization accompanying biotitic envelopes is quartz-calcite-molybdenite. Here two types of envelopes occur. One contains biotite which is considerably lighter than that associated with copper minerals. The other, which is younger, has a silicified envelope containing only a few percent of pale brown mica, presumably biotite or iron-rich phlogopite. The veins with biotitic envelopes generally cut those with actinolite envelopes where the two interesct. Quartz-calcite-molybdenite veins are later than bornite, chalcopyrite, and chalcopyrite-pyrite-bearing fractures.

K-feldspar

Potassium feldspar was not observed as a major hydrothermal phase in sedimentary rocks near the intrusion. In a few cases, intercepts of quartzite within a few meters of the intrusion resemble Stringham's (1953) descriptions of "granitized quartzite" which contain abundant biotite clots and streaks. A few specimens from the biotite zone collected within 30 m of the intrusive contact were stained to reveal the presence of K-feldspar, and only traces were found. However, it is possible that locally pervasive Late Stage sericitic and argillic alteration in quartzite near the stock has removed Main Stage feldspar.

In one unusual occurrence near the outer edge of the diopside zone, small clots (1 to 10 mm) of hydrothermal K-feldspar were found in sandy hornfels. They occur in association with irregular fractures which have very thin (0.5 mm) dark green actinolite envelopes, and a halo of such actinolite surrounds the K-feldspar.

Zoning of Main Stage

The mineral assemblages characterizing the various zones of the western contact aureole are summarized in Table 2. As described earlier, not all of the Early Stage zones may be present within any particular stratigraphic unit. A similar situation is true for Main Stage alteration of diopside hornfels, where locally the actinolite (+ biotite) envelope zone extends to the intrusion without the intervening pervasive actinolite and biotite zones.

The Main Stage alteration zones show considerable areas of overlap, not all of which are illustrated in Figure 7. Orbicules occur in areas of streaky actinolite, and envelopes occur in the inner part of the orbicule zone. The zone of biotite envelopes lies entirely within the inner part of the zone of actinolite envelopes. Here the biotite zone has clearly moved outward, encroaching on the actinolite zone.

Sulfides in the quartzite and interbedded thin limestone also show well-developed zoning (Fig. 8A). Pyrite is dominant in the orbicule zone. Within any particular lithology, the chalcopyrite : pyrite ratio increases as the intrusion is approached but does not show sharp changes from one alteration zone to another. However, biotite envelopes are associated principally with chalcopyrite, bornite, or quartz-calcite-molybdenite veins and not usually with pyrite. At depth and in the quartz-rich sedimentary sequences, pyrite eventually disappears, and sulfides consist of chalcopyrite, or, locally, chalcopyrite and bornite. An increase in the bornite : chalcopyrite ratio toward the stock is noted in some areas. Within 60 m of the intrusion, only traces of sulfides are present, and these are almost exclusively Late Stage pyrite. This decrease in sulfide abundance in the sedimentary rocks is very sharp and occurs over a few tens of meters.

Some thin beds near the outer edge of the sulfide-bearing zone have high chalcopyrite : pyrite ratios. These beds are apparent in Figure 8A near the center of the figure, about 250 m above the Yampa limestone. The inclusion of pyritic veins belonging to the Late Stage of alteration results in an overall abundance of pyrite equal to, or somewhat greater than, chalcopyrite. However, the chalcopyrite and some pyrite are present primarily as earlier disseminations in diopside hornfels, either in fresh diopside (Early Stage) or with small clots of actinolite (Main Stage). These occurrences suggest that during the Early and Main Stages of sulfide deposition chalcopyrite : pyrite ratios were relatively high, even at the outermost edges of mineralization.

Main Stage sulfide ratios are also very sensitive to lithology. The chalcopyrite : pyrite ratio increases as the presulfide detrital quartz : diopside ratio increases. Thus, hornfels beds, originally silty limestone, have a significantly lower chalcopyrite : pyrite ratio than adjoining quartzite beds. Most of the irregularity of the pattern of sulfide ratios in Figure 8A is due to these lithologic differences.

Locally, chalcopyrite veins may be observed which cut pyrite veins or rock containing earlier disseminated pyrite. These occurrences suggest the outward movement of sulfide zones, which is consistent with the inferred direction of movement of the silicate zones. However, these occurrences are rare, and most cross-cutting relationships indicate a decreasing chalcopyrite : pyrite ratio with time, or an inward collapse of sulfide zoning. Most of the pyritic veinlets also have actinolite envelopes and are believed to represent the late part of the Main Stage.

The abundance of sulfides in the contact aureole is illustrated in Figure 8B. The sulfide content of individual beds increases toward the stock, reaches a maximum, and then decreases. The orbicule zone contains generally less than 0.2 percent sulfides by volume; zones of envelope-controlled alteration contain the greatest quantity of sulfides not only as fracture fillings but also as disseminations and bedding-controlled clots.

The sulfide abundance of any particular bed is a direct function of its diopside content before actinolite alteration. This in turn depends on the original calcite : quartz ratio of the sedimentary rocks. Thus, quartz-poor beds have a higher total sulfide content but lower chalcopyrite : pyrite ratios than adjacent quartz-rich beds. The differences in chalcopyrite content and, therefore, copper grade tend to be minimized.

Magnetite and specular hematite are rarely observed in quartzite and thin silty limestone, in contrast with the relatively high abundance of these iron oxides in limestone skarn. In the thousands of meters of core examined, only three occurrences of hematite and 17 of magnetite were noted in quartz-rich rocks. All of these included pyrite and chalcopyrite as part of the assemblage and were associated with epidote or garnet in actinolized or biotized rocks.

Main Stage Alteration and Mineralization in Major Limestones

Andradite, diopside, and quartz, accompanied by magnetite, hematite, and copper-iron sulfides, represent the Main Stage of contact metasomatism in the Highland Boy and Yampa limestones. Garnetization expanded outward from the porphyry contact and locally overrode the Early wollastonite zone and impinged directly onto marble. Later garnet-destructive alteration which led to a variety of fracture-

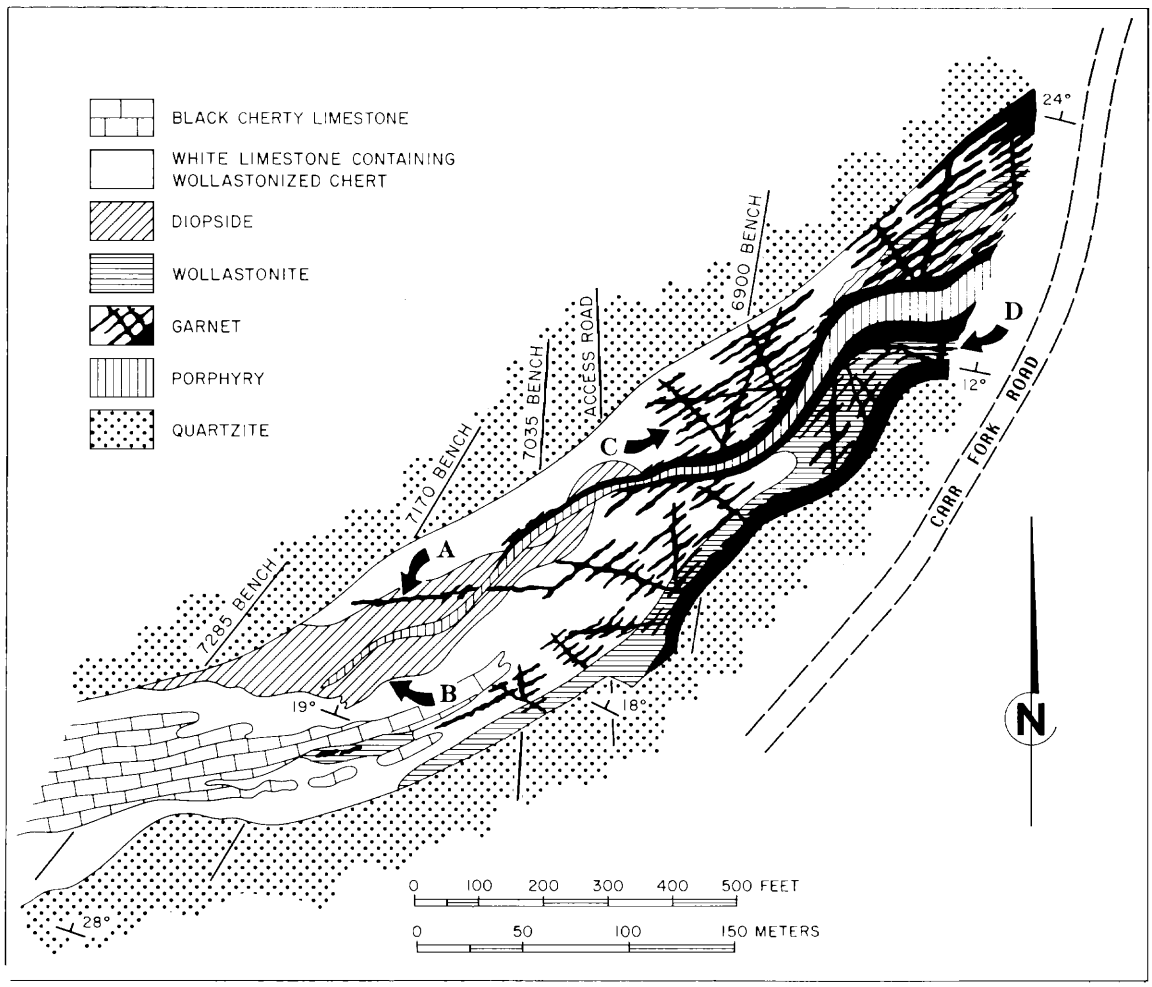

FIG. 10. Surface map of Yampa limestone showing extent of bleached limestone, diopside-calcite, wollastonite, and garnet. Development of garnet along veins and in bedding streaks is greatly simplified.

A. Garnet vein, composition $Ad_{28}Gr_{72}$, in diopside-calcite rock associated with idocrase, bornite, and chalcopyrite, near wollastonite.

B. Idocrase disseminated in diopside-calcite rock.

C. Location of Figure 12A.

D. Location of Figure 12B.

controlled actinolite-, carbonate-, and sulfide-bearing assemblages is included here as part of the Main Stage. Zoning of Main Stage alteration and mineralization is summarized in Figures 10 and 11.

Garnet

The processes by which the garnet zone developed are well illustrated in the transition from the garnet zone to the wollastonite zone. Garnetization first developed primarily along steep, crosscutting veins, rather than along a broad front (Fig. 10). The veins formed by replacement of wall rock rather than by fracture filling; garnet occurs either as disseminations or massive replacements a few centimeters wide in the walls of fractures. Veins occurring farthest from the stock in the wollastonite zone consist of dark, yellow-brown garnet in wollastonite, or pale buff, fine-grained garnet in diopside-calcite rock. One unit cell determination of garnet from the latter vein type indicated 72 mole percent grossularite (Table 4, no. 11) which is unusually aluminum rich for Carr Fork garnets. Both vein types contain chalcopyrite, bornite, and brown euhedral idocrase. Thirty to 60 m closer to the stock, some garnet-bearing veins contain specular hematite, quartz, calcite, actinolite, and chalcopyrite. Other veins showing the same mineralogy contain magnetite pseudomorphs after hematite.

Closer to the stock, garnet extends several meters out from fractures, preferentially replacing marble

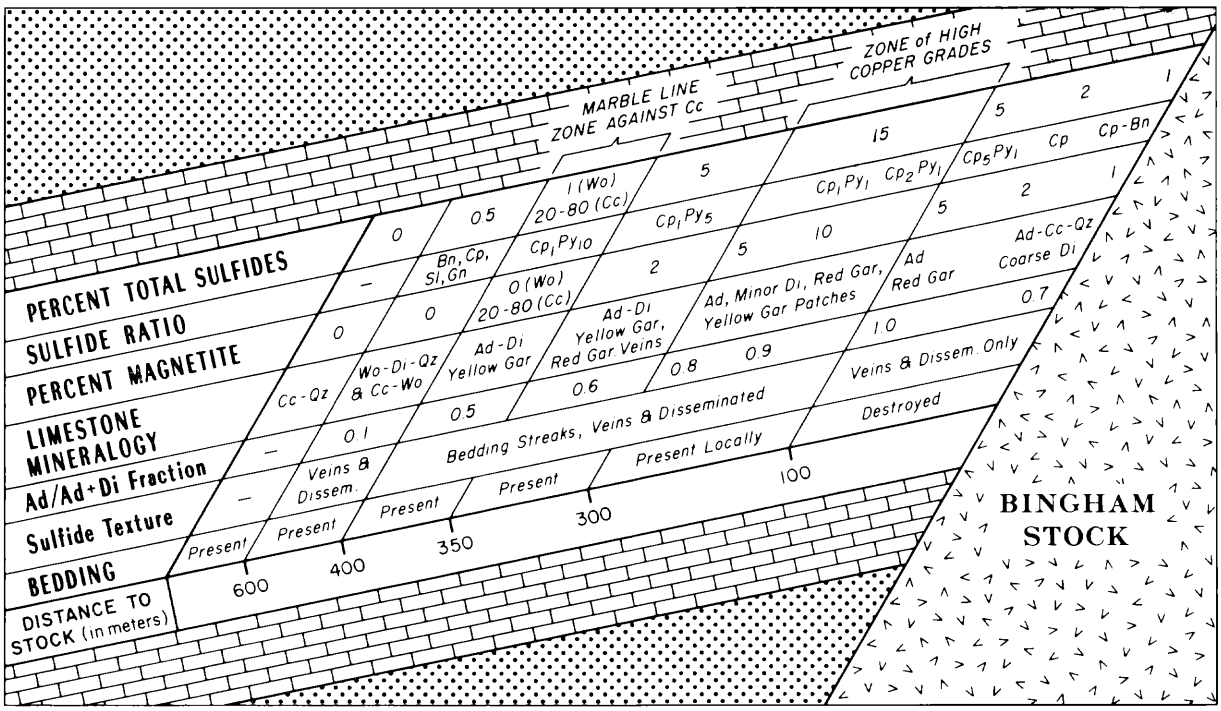

FIG. 11. Schematic zoning model for Highland Boy limestone, based on drill hole intercepts. Mineralogy is variable at the edge of garnetization, depending on whether garnet contacts wollastonite or calcite marble. Where marble is present, a marble contact-type orebody with high sulfide and magnetite content occurs. Abbreviations as in Table 2.

layers interbedded with wollastonite layers (Fig. 12). At the outer edge of the garnet zone, all marble and some wollastonite is replaced by garnet, and the rock consists of interlayered wollastonite and garnet (Fig. 12).

Abundant quartz-rich layers, comprising locally as much as 50 percent of the bed, are present in surface exposures of the garnetized Yampa limestone. The thickness and morphology of these layers are the same as those of chert layers in unaltered limestone. Similar layers are present in core from deep drilling but represent less than 10 percent of the volume of the garnetized limestone bed. However, both in the core and at the surface, no unaltered chert remains at the outer edge of the garnet zone; all chert was converted to wollastonite. Apparently these quartz-rich layers were once chert, then were converted to wollastonite, and later were replaced by glassy quartz during garnetization.

Four garnet samples from different environments and of different color were chosen as part of a suite of representative minerals for wet chemical analysis. The results, presented in Table 5, are discussed below in terms of mole percent andradite content calulated according to the method of Rickwood (1968). Analyzed garnets are very rich in the andradite end member; the compositions presumably reflect the low aluminum content of the sedimentary rocks as well as, more indirectly, the composition of the metasomatic fluid emanating from the area of the stock. The range of compositions from 98 mole percent andradite (Ad_{98}) to Ad_{92} is roughly correlative with color: red and brown garnets yield compositions of Ad_{98} and Ad_{97}, whereas yellow-green and gray-green garnets yield compositions of Ad_{92} and Ad_{95}. Garnets show a zoning in color in the major limestone beds from reddish brown near the stock to brown farther away, and finally to yellowish browns and greens in the outer wollastonite zone (Fig. 11); hence, the preliminary analytical results suggest that the andradite content decreases with distance from the stock.

Unit cell and refractive index measurements of the analyzed garnets suggest compositions which are 5 to 14 percent lower in andradite content than that obtained by chemical analysis. Most of the unit cell determinations of other garnets which were analyzed chemically probably yield results no better than this (Table 4). However, one group of determinations yields compositions ranging from Ad_{100} to about Ad_{103}. It appears that precision of the determinations is not the cause of deviations, but possibly minor components of the garnet may be responsible.

TABLE 4. Mole Percent Andradite in Carr Fork Garnets on the Basis of Chemical Analysis, Refractive Index, and Unit Cell

	Sample no.	Unit cell (A)	Refractive index	Mole % ad from R.I. & U.C.	Mole % ad chem. anal.	Color
1.	35-2540	12.005	1.872	90	94.6	red
2.	53-3880	11.993	1.868	84	96.4	brown
3.	33-82-349	12.001	1.858	81	90.9	yellow-green
4.	56-5500	12.007	1.863	82	94.4	gray-green
5.	63-3368	12.051	1.884	102		brown
6.	67-562	12.052	1.885	102		yellow
7.	67-613	12.047	1.886	103		yellow
8.	67-788A	11.976	1.843	62		light green
9.	67-788B	12.054	1.883	100		brown
10.	712	11.850		0		pale buff
11.	717	11.905		28		pale yellow-brown
12.	736	11.925		36		pale buff
13.	738	12.010		80		yellow-brown
14.	740	12.020		85		pale green
15.	801	12.015		82		yellow-brown
16.	922	12.020		85		yellow-brown
17.	930	11.985		68		greenish-brown
18.	945	12.015		82		pale buff
19.	952	12.010		80		light green
20.	970	11.990		70		yellow-brown

Notes: Precision: 1–9, UC ± 0.001A, RI ± 0.001 − 0.005; 10–20, UC ± 0.005A.
1. Highland Boy limestone, 120 m from porphyry, associated with magnetite, chalcopyrite, and diopside.
2. Yampa limestone, 120 m from porphyry, associated with magnetite, chalcopyrite, diopside.
3. Yampa limestone, 3300 level Apex mine, massive garnetite close to wollastonite.
4. Yampa limestone, 300 m from porphyry, associated with pyrite, chalcopyrite, magnetite.
5. Highland Boy limestone, near highest copper grades.
6–9. Tilden series, outer garnet zone near wollastonite; 8 forms patches which are veined by 9.
10–20. Surface samples, from the fringes of the garnet zone.
10. Yampa limestone, xenolith in narrow dike, associated with idocrase and epidote.
11. Yampa limestone, garnet vein in wollastonite near diopside-calcite rock, associated with idocrase and chalcopyrite.
12. Highland Boy limestone, endoskarn dike.
13. " " " , in marble with chalcedony.
14. " " " , massive garnetite with actinolite.
15. " " " , quartz vein in diopside hornfels.
16. " " " , near wollastonite-marble, porphyry dike.
17. Yampa limestone, interbanded wollastonite and garnet.
18. " " , near wollastonite, associated with clay, chalcedony, oxidized copper minerals.
19. Yampa limestone, adjacent to wollastonite, associated with oxidized copper minerals.
20. " " , basal streak of garnet, just below wollastonite.

Correlation of properties with analyses of garnets from Deer et al. (1966) indicates similar deviations.

Notwithstanding the inherent difficulties with the determinations using combined X-ray and refractive index methods, these methods may be used to give a rough indication of relative andradite content. The two garnets (nos. 10 and 12) from dikes are aluminous as would be expected, and garnet from one vein near the outer edge of silication in limestone has a very high grossularite content (no. 11). Patches of green garnet with an apparent composition of Ad_{62} (no. 8) are veined by Ad_{100} (no. 9). Aside from these results, it appears that all other garnets have a relatively high andradite content in the range Ad_{68} to Ad_{100}. It is particularly surprising that the majority of garnets from the outer garnet-bearing diopside wollastonite zone in the Tilden series are apparently pure andradite (nos. 6 through 9), whereas garnets from the outer edge of the garnet zone in the major limestone beds contain less than 85 mole percent andradite (nos. 11 and 13 through 20).

Diopside

Fine-grained diopside is nearly ubiquitous in the garnet zone. Near the outer edge of the garnet zone and in hornfels beds at the hanging-wall transition from limestone to quartzite (Fig. 1), abundant diopside occurs as monomineralic layers interbedded with, and veined by, garnet. Within the limestone beds, these diopside layers and patches decrease in thickness and abundance toward the stock. On a microscopic scale, diopside grains 1 to 5 μm in size are disseminated in garnet locally.

From the outer zones toward the stock, a gradation in color of diopside is apparent from pale brown to darker grayish and greenish brown, presumably reflecting a change in iron content. Considerable variability in pyroxene composition is indicated by the analyses presented in Table 6, although lack of sufficient data prevents any definitive statement on trends in pyroxene composition.

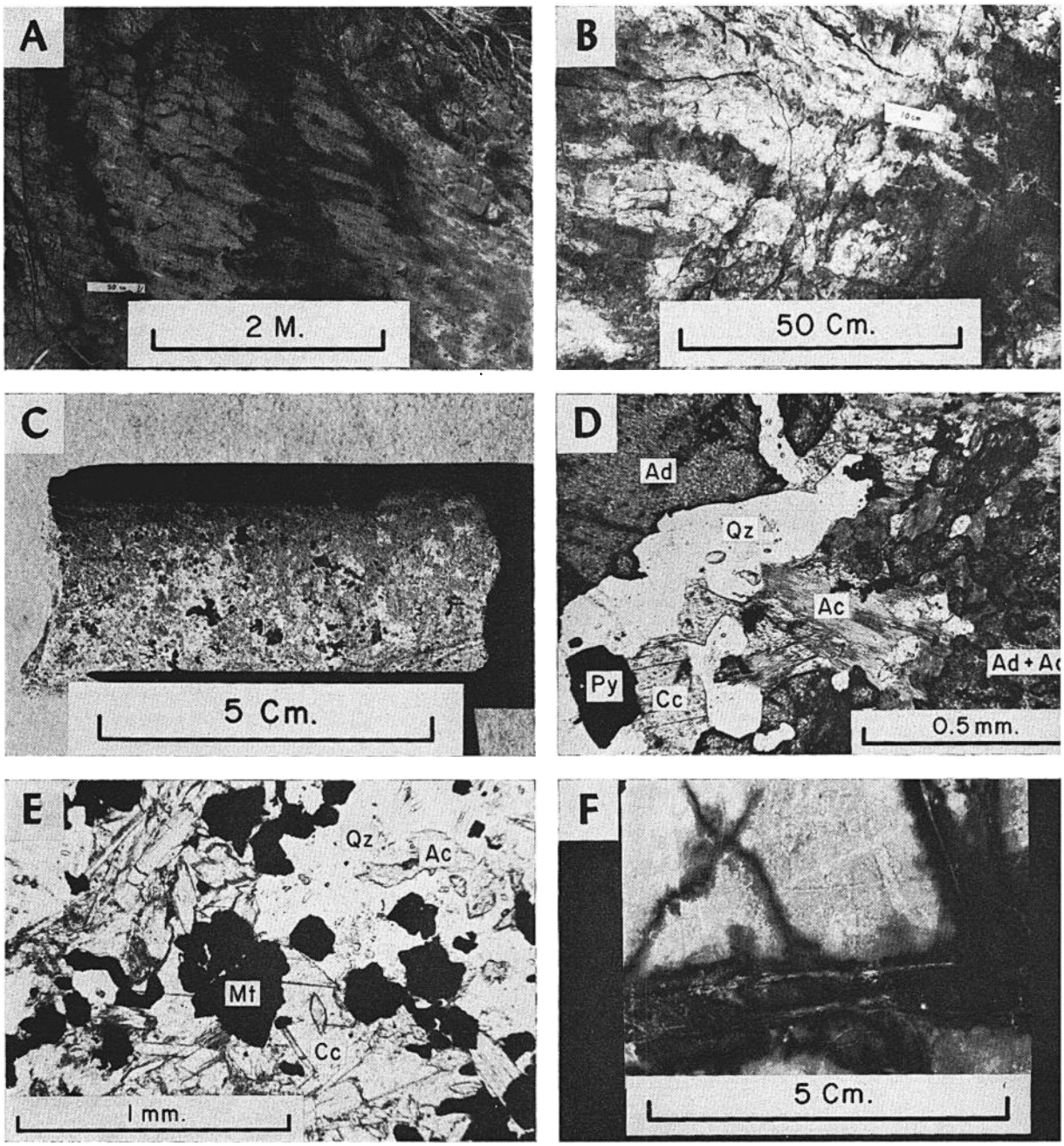

FIG. 12. A. Steep oxidized sulfide veins with andradite envelopes (dark material) showing selective replacement of calcite marble layers which alternate with wollastonite-bearing chert layers in Yampa limestone outcrop.

B. Andradite layers (dark) alternating with wollastonite-bearing chert, Yampa limestone outcrop. Carr Fork road near the Kennecott-Anaconda property boundary.

C. Garnet-destructive alteration. Black spots are magnetite, white is calcite-quartz, and background gray is andradite.

D. Photomicrograph in transmitted light, showing quartz-calcite-magnetite-actinolite veinlet cutting andradite. Grains of diopside enclosed in andradite are altered to actinolite.

E. Photomicrograph in transmitted light, showing quartz-calcite-magnetite-actinolite assemblage in an area of andradite destruction.

F. Typical silicification-pyritization (black envelope) of calc-silicates along fractures, associated with high gold assays in diopside-rich quartzite.

Actinolite

Actinolite is a minor phase in the garnet zone and does not appear as part of the dominant andradite-diopside assemblage present throughout most of the garnetized limestone beds. Rather, actinolite commonly occurs near the outer edge of the garnet zone as finely fibrous crystals disseminated in garnet and in garnet-bearing veins in the wollastonite zone. In the latter occurrence, actinolite does not occur in contact with wollastonite and appears to be contemporaneous with garnet. Massive garnet in the outcrops of both the Yampa and Highland Boy limestones at the surface also contains local interstitial actinolite; a common assemblage consists of actinolite-garnet-quartz-hematite ± calcite ± magnetite.

Actinolite also is a locally important alteration product of garnet and diopside adjacent to later sulfide veinlets and patches. These occurrences are discussed in a later section.

TABLE 5. Chemical Analyses of Garnets

	1	2	3	4
SiO_2	35.06	35.86	36.20	37.28
TiO_2	0.00	0.07	0.00	0.13
Al_2O_3	1.15	0.69	1.84	0.97
Fe_2O_3	31.46	30.12	28.65	27.29
FeO	0.66	0.55	0.15	0.18
MnO	0.26	0.24	0.21	0.21
MgO	0.12	0.26	0.32	1.63
CaO	31.93	32.14	32.11	32.29
Na_2O	0.07	0.00	0.09	0.04
K_2O	0.03	0.01	0.03	0.01
S	0.00	0.00	0.02	0.01
H_2O^+	0.34	0.34	0.06	0.10
Total	101.08	100.28	99.68	100.14
$n(\pm 0.003)$	1.872	1.868	1.858	1.863
a(A) (± 0.001A)	12.0054	11.9926	12.001	12.0067
Number of cations on basis of 24 oxygens				
Si	5.846	5.991	6.061	6.173
Ti	0.000	0.009	0.000	0.016
Al	0.226	0.136	0.363	0.189
Fe^{+3}	3.947	3.786	3.609	3.400
Fe^{+2}	0.092	0.077	0.021	0.025
Mn	0.037	0.034	0.030	0.030
Mg	0.030	0.064	0.080	0.402
Ca	5.704	5.753	5.759	5.728
H	0.376	0.378	0.067	0.110
Total	15.976	15.945	15.990	15.990
Molecular % end members				
Andradite	97.6	96.9	91.9	94.7
Pyrope	0.5	1.1	1.3	5.3
Spessartine	0.6	0.6	0.5	0.0
Hydrogrossularite	0.0	0.1	0.3	0.0
Grossularite	0.0	0.0	5.6	0.0
Almandite	1.3	1.3	0.4	0.0
% cations allocated	95.9	96.5	98.6	89.3

Notes: Analyses by James Cardwell, wet analytical methods. Molecular end members calculated by method of Rickwood (1968).

1. Red garnet, top of Highland Boy limestone, associated with diopside, magnetite, and chalcopyrite, 120 m from porphyry.
2. Brown garnet, top of Yampa limestone, associated with diopside, magnetite, and chalcopyrite, 120 m from porphyry.
3. Yellow-green garnet, Yampa limestone, massive garnetite close to wollastonite zone.
4. Gray-green garnet, Yampa limestone, associated with chalcopyrite, pyrite, and magnetite, 300 m from porphyry.

TABLE 6. Chemical Analyses of Pyroxenes

	1	2	3
SiO_2	54.48	51.97	51.90
TiO_2	0.11	0.00	0.04
Al_2O_3	0.14	0.02	0.00
Fe_2O_3	0.90	3.01	4.76
FeO	0.56	2.46	7.18
MnO	0.02	0.14	0.25
MgO	17.47	16.78	11.53
CaO	24.63	22.94	23.38
Na_2O	0.13	0.28	0.45
K_2O	0.02	0.06	0.07
P_2O_5	—	0.00	—
S	0.02	0.02	0.00
$+H_2O$	0.62	0.37	0.20
Total	99.10	98.05	99.76
−O correction for S	0.01	0.01	0.00
Total	99.09	98.04	99.76

Numbers of cations on basis of 6 oxygens

	1		2		3	
Si	1.98		2.11		1.96	
Ti	0.00	1.99	0.00	2.12	0.00	1.96
Al	0.01		0.01		0.00	
Fe^{+3}	0.02		0.08		0.14	
Fe^{+2}	0.02	0.98	0.08	1.09	0.23	1.03
Mn	0.00		0.00		0.01	
Mg	0.94		0.93		0.65	
Ca	0.96		0.92		0.95	
Na	0.01	0.97	0.02	0.94	0.03	0.98
K	0.00		0.00		0.00	
H	0.15		0.09		0.03	
Total	4.09		4.24		4.00	
Fe/Fe + Mg	0.04		0.15		0.36	

Analyses by James Cardwell. Wet analytical methods.

1. White diopside, from diopside hornfels in the quartzite sequence, containing 10% apatite, green actinolite envelopes on fractures, and 0.5–1% cp_5py_1 on the fractures. Sparse inner biotite envelopes. From upper part of the biotite zone, 120 m from porphyry.
2. Light yellow-green diopside, from top of Highland Boy limestone, associated with calcite, quartz, and chalcopyrite. From a 0.6 m-thick layer below 1 m of massive light green actinolite, and above dark red garnetite (see garnet no. 1, Table 5). 120 m from porphyry.
3. Medium dark green diopside, from the Yampa limestone, associated with pale green garnetite (see garnet no. 4, Table 5), chalcopyrite, and magnetite. 300 m from porphyry.

Early magnetite and hematite

Magnetite in the contact aureole is confined almost entirely to the two major limestone units, and its

abundance depends on elevation and distance from the stock. At any given elevation, the magnetite content rises sharply from the stock to a maximum at the otuer edge of the low sulfide zone, then decreases gradually toward the outer edge of silication (Fig. 11). Magnetite abundance is highest at greatest depth, where some whole-bed intercepts average 25 volume percent; it diminishes toward the surface, where it comprises less than one percent of the skarn. A large part of the magnetite encountered in deep drilling appears to have replaced garnet directly without visibly altering adjacent grains of relict garnet. Such magnetite usually occurs as nearly pure lenses and irregular rounded masses in garnet; some unaltered diopside also is usually present. These relations suggest that magnetite represents the end-product of the trend toward iron enrichment during zoned skarn formation, which initially resulted in replacement of diopside by andradite.

At the surface, where a wollastonite zone is well developed, no magnetite occurs at the outer edge of the garnet zone. Magnetite would not be expected to form because it is incompatible with wollastonite at the T-f_{O_2} conditions of skarn formation in the Bingham district. Studies of fluid inclusions indicate that quartz veins from the Bingham stock formed over a range of temperatures from 725° to 400°C (Roedder, 1971; Moore and Nash, 1974). Presumably, the Carr Fork skarns formed at lower temperatures than the maximum indicated by veins in the stock. At such temperatures the assemblage wollastonite-magnetite is stable only at oxygen fugacities which are significantly lower than the andradite-hedenbergite-quartz-magnetite buffer (Gustafson, 1974). The presence of andradite-quartz-magnetite through most of the depositional history, and the absence of hedenbergite, indicates that oxygen fugacities remained at relatively high levels. Thus, iron-bearing solutions reacted with wollastonite to form andradite rather than magnetite.

At greater depths, where higher P_{CO_2} presumably inhibited the development of a wollastonite zone, magnetite is found in high concentrations at the contact between the garnet zone and marble.

Specular hematite occurs in veinlets, streaks, and masses up to 3 m thick adjacent to porphyry dikes and at the contact between silicates and marble in the old Highland Boy mine. In these occurrences hematite is associated with pyrite, calcite, garnet and, locally, actinolite. In a few places hematite occurs with magnetite and quartz in addition to all of the above minerals. Here magnetite is always partly pseudomorphous after specular hematite.

A striking difference in abundance of specular hematite was noted between the old Highland Boy mine area near the surface and the areas of deep drilling 500 to 1,500 m to the north and about 1,000 m deeper. Locally, massive specular hematite occurs in the old Highland Boy mine, but at depth, specular hematite occurs only in thin late veinlets, and magnetite is the dominant early iron oxide. However, lack of exposures precludes a more complete knowledge of the three-dimensional distribution of magnetite and hematite.

In addition to the above occurrences, in which iron oxides appear to be contemporaneous with the main period of zoned, anhydrous skarn formation, magnetite also occurs with carbonates, quartz, and actinolite in later, skarn-destructive alteration. These occurrences are discussed in a later section.

Early sulfides

Sulfides in the ore zones commonly follow veins which crosscut bedding, are associated with demonstrable alteration of garnet, or occur in textures whose age relations are unclear. Thus, it is difficult to find occurrences that indicate that sulfides formed contemporaneously with diopside garnet. In the area of highest copper grades the presence of chalcopyrite interstitial to euhedral fresh garnet crystals or in bedding streaks with fresh garnet and diopside may be indicative of early sulfide deposition. However, an alternate interpretation is that chalcopyrite replaced calcite which was interstitial to garnet. Bedding streaks are similarly ambiguous. The best evidence that some chalcopyrite accompanied garnet comes from the outer edges of garnetization, where chalcopyrite is associated with garnet veinlets or with disseminated garnet in wollastonite or diopside rock.

Epidote

Major occurrences of epidote are localized near igneous contacts. Replacement of aluminous garnet by epidote adjacent to igneous dikes in the Highland Boy mine has already been mentioned. Epidote also has been noted in several core intercepts, where it occurs in epidote-garnet-actinolite-calcite-pyrite skarn adjacent to porphyry. The writers mapped an exposure of epidote-quartz-diopside-actinolite skarn between garnetized Yampa limestone and quartz monzonite in the Utah Copper pit; as discussed in the next section, this epidote-bearing rock is probably an endoskarn. Aside from these occurrences, epidote occurs only locally and in small concentrations. Late epidote-bearing veinlets cut garnetized limestone and usually contain specular hematite, calcite, pyrite, and magnetite pseudomorphs after specular hematite.

Endoskarn

In the Carr Fork area, endoskarn is well developed in quartz monzonite adjacent to garnetized limestone but is not present at contacts with quartzite. From biotitized intrusive rock toward exoskarn, the first noticeable change, a few meters from the contact, is the appearance of hydrothermal actinolite, which increases in abundance as biotite decreases. Diopside then appears at approximately the point where biotite is no longer present. Within a few centimeters from the exoskarn, pale pinkish garnet appears as irregular amoeboid masses replacing all igneous minerals, and epidote occurs locally. Sphene is present throughout the endoskarn. In many places, the precise intrusive contact is obscure and may lie at any point within a zone up to a meter in width. Usually, the sphene content drops sharply near the contact, and calcite becomes more abundant in the exoskarn. A few centimeters into the exoskarn, garnet becomes more abundant and diopside decreases.

The contact between quartz monzonite and the Yampa limestone was mapped in the Utah Copper pit. Here the endoskarn followed the same pattern as observed in core, zoned toward the contact with the sequence biotite, actinolite, diopside, and garnet, except that epidote and quartz also are abundant in the zones of diopside and garnet. The area near the Yampa-quartz monzonite contact contains disseminated chalcopyrite and magnetite and is traversed by numerous quartz-chalcopyrite veins having biotite envelopes in the actinolite zone, actinolite envelopes in the diopside zone, and diopside envelopes in the garnet zone. Some veins also have multiple envelopes, such as inner biotite and outer actinolite in the diopside zone.

Zoning of minerals at igneous contacts and relations between veinlets in the stock and veinlets in the skarn can be used to interpret the age relations between skarn formation and the evolution of alteration-mineralization in the Bingham stock. The relations described above suggest that endoskarn in quartz monzonite is not related in time to the emplacement of quartz monzonite. Rather, the facts that both endoskarn and garnetized limestone are restricted to areas close to quartz monzonite porphyry, and that a close relation exists between endoskarn and the presence of mineralized veinlets related to the potassic stage of alteration in the stock, suggest that the endoskarn is a product of Main Stage skarn formation related to the emplacement of quartz monzonite porphyry. Main Stage fluids, concentrated along the contact of the quartz monzonite, affected the bimetasomatic transfer of calcium into quartz monzonite and of magnesium and iron into limestone, producing the observed mineral zoning pattern. The main effect in the stock was the replacement of magmatic biotite by actinolite due to the relatively high activities of calcium in the fluid. At a slightly later time, during the main period of biotite-orthoclase alteration in the stock's interior, quartz-chalcopyrite veinlets introduced secondary biotite in the innermost endoskarn zone and extended into the outer endoskarn, where the associated alteration envelopes changed to actinolite and locally diopside. Veinlets at contacts between diopside hornfels and igneous rocks, discussed in a previous section, also indicate that biotite and actinolite are contemporaneous alteration products related to Main Stage chalcopyrite mineralization in rocks of relatively low calcium content.

Correlation of Main Stage in quartzite and major limestone beds

The postmetasomatic mineralogical compositions of quartzite and thick limestone beds present strong contrasts: limestone is replaced primarily by garnet and contains large amounts of diopside, sulfides, and magnetite, whereas quartzite consists primarily of quartz and abundant diopside and lesser amounts of actinolite and sulfides. Both lithologies were presumably subject to the same P-T conditions and were invaded by the same solutions. How, then, is the mineralogy of the two types related?

In limestone, garnet replaced wollastonite, calcite, and diopside, whereas in quartzite, actinolite replaced diopside. Although exposures are not sufficient to conclusively document the age relations of actinolite and garnet in these two lithologies, the evidence from numerous drill holes which pass from silty diopside hornfels to garnetized limestone suggests that some actinolite alteration and garnetization are broadly contemporaneous. Chalcopyrite-pyrite veinlets, which bear actinolite envelopes in diopsidic quartzite and silty diopside hornfels, continue into the upper portions of limestone beds where the vein fillings include magnetite; vein envelopes consist of magnetite or magnetite-garnet, and actinolite disappears. Farther into the limestone bed, garnet envelopes and patches coalesce.

These relations are portrayed graphically on the Ca-Mg-Fe projection of Figure 13, which illustrates the mineral compatibilities prevailing during the main period of silication (Einaudi, 1975a). Limestone beds containing calcite, wollastonite, and minor diopside plot near the Ca apex, whereas diopside-bearing quartzite plots at the diopside composition because silica is not represented independently. From the diagram it may be seen that if iron is added to limestone and the Ca/Mg ratio remains approximately constant, the iron content of diopside first increases,

then andradite appears. In quartzite, however, amphibole is the first new phase to appear. Thus, iron metasomatism in quartzite resulted in the formation of actinolite, but in limestone andradite was formed. Continued addition of iron to the limestone resulted in the formation of the assemblages andradite-diopside-magnetite and andradite-magnetite close to the stock. In quartzite and thin silty limestone beds, pyrite rather than magnetite accompanied actinolite.

Alteration of anhydrous skarn

The development of zoned limestone skarn by Fe metasomatism was followed by alteration of diopside and andradite to a variety of carbonate- and actinolite-bearing assemblages accompanied by major amounts of sulfides. In contrast with earlier skarn-forming events, which involved dominantly the introduction of base metal cations and the formation of simple coarse-grained assemblages of a few phases, these later events can be interpreted as the result of hydrolysis, and recarbonation of previously formed calc-silicates, and partial leaching of calcium. The resulting assemblages for the most part are complex, fine-grained intergrowths; relicts of early skarn silicates and textures are commonly found.

The alteration assemblages display a dependence on the original garnet: diopside ratio of the skarn: late actinolite is more abundant where diopside was associated with garnet, toward the outer edge of the garnet zone; near the intrusion, where the garnet: diopside ratio was high, actinolite is less common.

Three types of late actinolite occurrences were noted. In one, pyrite-chalcopyrite veinlets with actinolite envelopes cut mixtures of garnet, diopside, and quartz. In the second, veins and patches of calcite, quartz, and actinolite occur in garnet and appear to have resulted through alteration of diopside rather than garnet (Fig. 12D). The third type, which is relatively more common, consists of patches or bedding streaks of quartz, calcite, actinolite, and magnetite; garnet and diopside are entirely destroyed (Fig. 12E). Chalcopyrite-actinolite intergrowths are commonly developed in such patches and locally magnetite is replaced by pyrrhotite.

In areas where andradite was the dominant skarn mineral and diopside is absent, the major alteration minerals include quartz, carbonates, iron oxides, and sulfides. The presence of patchy intergrowths of calcite, quartz, and magnetite in garnet (Fig. 12C) and granular calcite-quartz-magnetite pseudomorphs of garnet suggest the following reaction, written to conserve all nonvolatile components among the solids:

$$3Ca_3Fe_2Si_3O_{12} + 9CO_2 \rightleftharpoons 9CaCO_3 + 9SiO_2 + 2Fe_3O_4 + \tfrac{1}{2}O_2$$

andradite — calcite — quartz — magnetite

Various lines of reasoning suggest, however, that the above reaction does not adequately express the process that occurred: (1) the pseudomorphic relations suggest that the reaction proceeded at constant volume, but the above requires a two-fold increase in volume; (2) on the scale of individual patches of reaction products, the minerals are not present in the proportions expected from this reaction; and (3) the low abundance or common absence of calcite in silicified andradite skarn suggests that calcium is leached. On this basis, the following reaction more closely expresses the process of garnet destruction, at approximately equal volumes of the solids:

$$3Ca_3Fe_2Si_3O_{12} + 3HCO_3^- + 15H^+ \rightleftharpoons 3CaCO_3 + 9SiO_2 + 2Fe_3O_4 + 6Ca^{++} + 9H_2O + \tfrac{1}{2}O_2$$

In addition to magnetite, some intergrowths of calcite and quartz in garnet contain other iron-bearing minerals, including hematite, siderite, pyrite, chalcopyrite, and bornite.

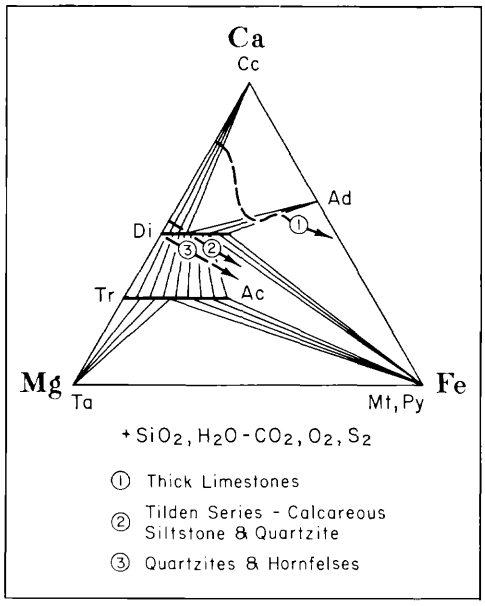

FIG. 13. The system Ca-Mg-Fe-Si-H_2O-CO_2-O_2 projected through quartz and volatiles, showing schematic metasomatic paths for different bulk compositions. The assemblages shown are those observed for the bulk of the rocks during Main Stage silication. Approximate average quartz contents for the three paths are 1, 25%; 2, 50%; 3, 80%. Abbreviations as in Table 2.

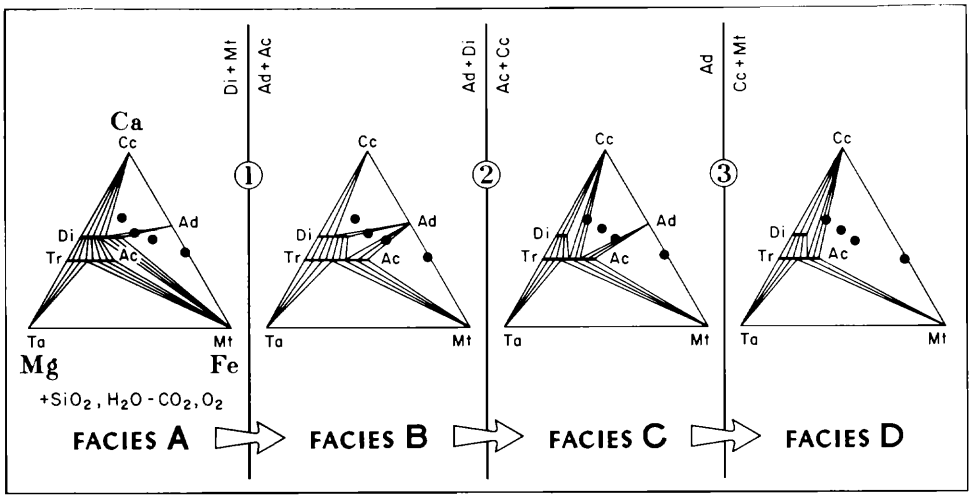

FIG. 14. Facies of the system Ca-Mg-Fe-Si-H_2O-CO_2-O_2 at temperatures below wollastonite stability projected through SiO_2 and volatiles. Assemblages produced by reactions accompanying ore deposition in garnetized limestone are indicated by black circles. Location of black circles in terms of Ca-Mg-Fe proportions is schematic. Quartz is present in all assemblages and additional quartz is produced on the right-hand side of reactions 2 and 3. Abbreviations as in Table 2.

It is significant that no aluminous minerals were found in these retrograde assemblages. In districts where garnets are known to be aluminous, such as at San Pedro, New Mexico, chlorite is a common mineral accompanying quartz, calcite, and specular hematite (Atkinson, 1976). In other cases, replacement by epidote is observed (Atkinson, 1976; Nielsen, 1970; Morgan, 1975). The lack of such aluminous minerals at Carr Fork is a further indication that the majority of the garnet is nearly pure andradite. However, adjacent to dikes in the Highland Boy mine, where the garnet may be relatively rich in the grossularite component (nos. 10 and 12, Table 5), garnet is altered to epidote.

Although the alteration reactions, particularly those involving the production of actinolite, are difficult to specify, a few generalizations can be made. The above observations on alteration of garnet-diopside skarn suggest that Fe-bearing diopside was less stable than andradite during the alteration process; no occurrences were noted in which garnet was altered and diopside remained fresh. A key assumption in the following discussion is that the actinolite produced by alteration of diopside was in equilibrium with the associated, unaltered, garnet. If this is the case, then the tie lines illustrated in Figure 13 underwent successive changes during alteration, which led first to the appearance of a stable andradite-actinolite tie line and eventually to the disappearance of andradite. These changes in compatibilities are illustrated in Figure 14, a two-dimensional representation of the system Ca-Fe-Mg-Si-H_2O-CO_2-O_2 that is achieved by projecting phase compositions through SiO_2 and volatiles onto the triangle Ca-Fe-Mg. Such a projection is valid for analysis of Carr Fork rocks because of the presence of quartz in all assemblages and the general lack of aluminum in silicates. Facies A (Fig. 14), defined by the assemblage andradite-diopside-magnetite-quartz, is the most common facies observed in garnetized limestones. Facies B and C, although not abundantly represented, are indicated by the later association of actinolite with andradite-diopside-quartz and andradite-calcite-quartz. Facies D, defined by the presence of actinolite-magnetite-calcite-quartz, is common, particularly where copper grades are high.

The reactions which relate the facies of Figure 13 may be expressed as follows:

$$5[CaFeSi_2O_6] + 2/3Fe_3O_4 + SiO_2 + H_2O + 1/6O_2$$
(in clinopyroxene) magnetite quartz

$$\rightleftharpoons Ca_3Fe_2Si_3O_{12} + [Ca_2Fe_5Si_8O_{22}(OH)_2] \quad (1)$$
andradite (in actinolite)

$$Ca_3Fe_2Si_3O_{12} + 3[CaFeSi_2O_6] + H_2O + 4CO_2$$
andradite (in clinopyroxene)

$$\rightleftharpoons [Ca_2Fe_5Si_8O_{22}(OH)_2]$$
(in actinolite)

$$+ 4CaCO_3 + SiO_2 + 0.5O_2 \quad (2)$$
calcite quartz

$$3Ca_3Fe_2Si_3O_{12} + 9CO_2 \rightleftharpoons 9CaCO_3 + 9SiO_2$$
andradite calcite quartz

$$+ 2Fe_3O_4 + 0.5O_2 \quad (3)$$
magnetite

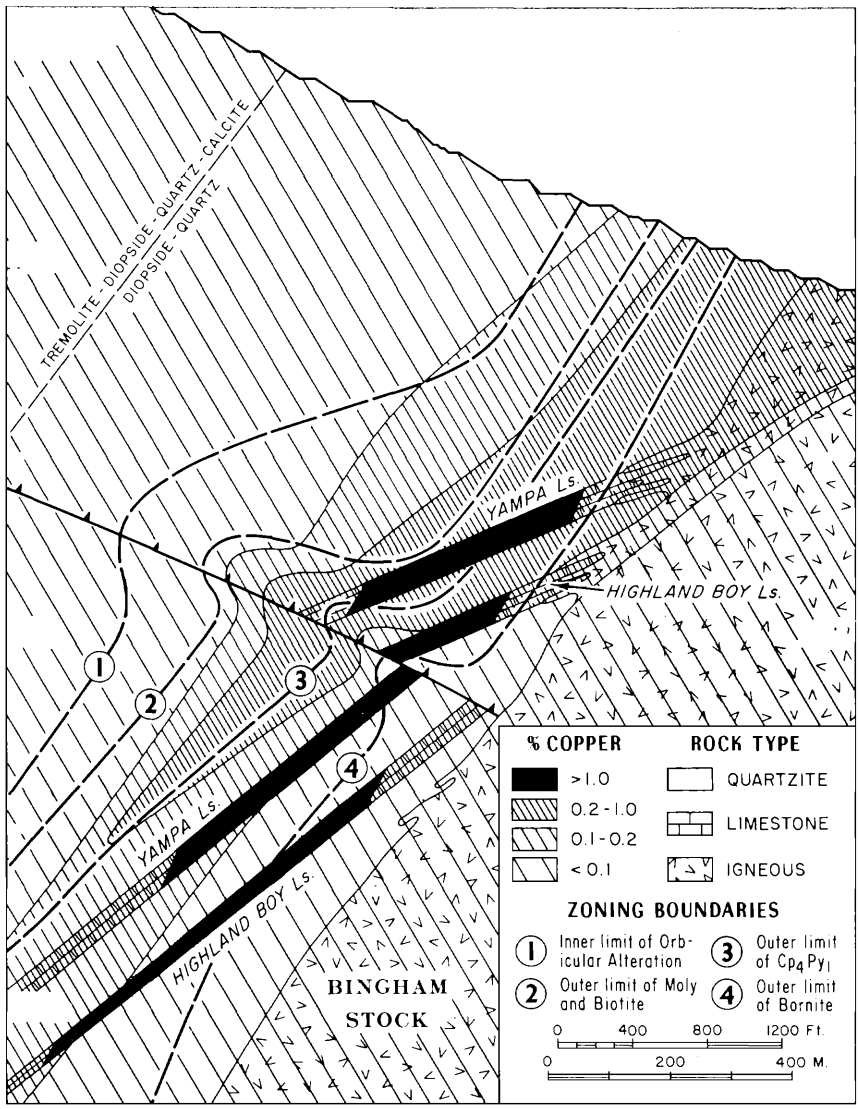

FIG. 15. Northwest cross section looking northeast, illustrating copper grades of quartzite, limestone, and the Bingham stock, and their relation to important zonal boundaries.

A model for the progressive change in the physicochemical environment which led to alteration of garnet and diopside must be compatible with the conclusion that the three reactions listed all were passed in the right-hand direction. This constraint rules out changes in X_{CO_2} or f_{O_2} as the dominant controls on alteration; for example, a decrease in X_{CO_2} or an increase in f_{O_2} drives reaction 1 to the right and reactions 2 and 3 to the left. However, for the case when both f_{O_2} and X_{CO_2} are constant or nearly so, the facies sequence A-B-C-D represents a trend toward decreasing temperature (Einaudi, 1975b). A thermal decline is therefore proposed as the dominant cause of alteration of earlier anhydrous skarn.

Zoning of sulfides

As in the quartzite and thin limestone sequences, sulfide assemblages in the major limestone beds are zoned (Fig. 11). Near the intrusion, disseminated sulfides consist primarily of chalcopyrite with local bornite. Pyrite, associated with chalcopyrite, becomes more abundant away from the intrusion, and bornite reappears with chalcopyrite and sphalerite in the outer wollastonite zone. Within 60 m of the porphyry contact the Main Stage sulfide zoning pattern is disrupted by Late Stage effects; the sulfide content of the garnetized limestones is greatly reduced and pyrite is present in association with strong clay alteration of calc-silicates.

Copper Distribution

The districtwide configuration of disseminated and stockwork copper mineralization has been described by James (1971) as an inverted cup-shaped volume which is draped over a low-grade core zone; this volume cuts across igneous and sedimentary rocks contacts. Grade boundaries in the quartzite sequence at Carr Fork substantiate this general model and show that the northwest side of the cup-shaped volume tapers downward but extends to great depths (Fig. 15). At an elevation of 3,000 feet, or 700 m below the present pit bottom, the zone of greater than 0.2 percent copper is wholly within the quartzite and located about 350 m from the stock, which itself contains less than 0.1 percent copper.

As a consequence of this geometry, copper grades rise to a maximum and then decrease outward from the porphyry at any given elevation in the quartzite sequence or within a given limestone bed. However, the grades are much higher in the limestone beds due to their more favorable initial composition. The position of the maximum grade in limestone does not coincide with that in quartzite but lies about 100 m closer to the intrusion. This is believed to be due to the lower permeability of limestone and to its effect as a chemical "sink" which is capable of precipitating large quantities of certain elements carried by hydrothermal solutions.

The copper distribution in the major skarn beds is usually erratic in detail, reflecting the occurrence of narrow bedding streaks and crosscutting veins of higher grade. Consequently, in order to determine the overall grade distribution, the average copper grade was computed for the entire thickness of each limestone bed intercept. Plots of whole-bed averages versus distance to the intrusion are illustrated in Figure 16 for elevations of 900 to 1,300 m. Data from lower elevations yield similar curves which are progressively shifted away from the contact and whose copper grade maxima are progressively lower with increasing depth. Higher grades in the Highland Boy limestone may reflect in part its lower stratigraphic position where it was more accessible to mineralizing solutions, assuming that these fluids were dominantly moving in an upward and outward direction. The grade distribution appears to be independent of thickness of limestone units. Observed thicknesses vary as much as four-fold due to stratigraphic thinning in some areas and tectonic thickening due to flowage into the trough of the Bingham syncline; nonetheless, copper grades maintain their systematic relation with respect to distance from the stock.

The systematic grade distribution reflects the presence of high permeability in the enclosing quartzite sequence, which allowed uniform entry of hydrothermal fluids, and the absence of highly variable original lithology, which would have influenced fluid-wall-rock reactions and hence ore deposition. The lack of local structural and lithological control during Main Stage skarn formation is reflected not only in the systematic grade distribution but also in the overall zonal distribution of mineral assemblages.

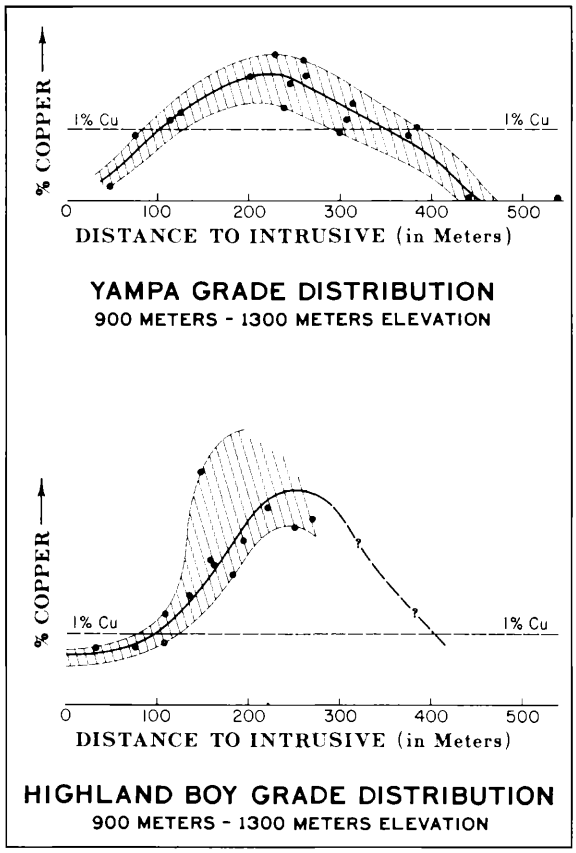

FIG. 16. Relation between copper grades in major limestone beds and distance to the Bingham quartz monzonite porphyry.

Late Stage Argillic Alteration

Late Stage alteration of skarn involves primarily the minerals chlorite, montmorillonite, "sericite" (muscovite and hydromuscovite), and talc, accompanied by pyrite. It is concentrated near the contact with the stock at higher elevations.

Chlorite

Chloritic alteration, accompanied by pyrite and chalcopyrite, is localized along fractures adjacent to the stock at higher elevations. In hornfels and quartzite, chlorite replaced actinolite or biotite in the centers of reopened veinlets or occurs along fractures which cut older actinolite or biotite veinlets. In

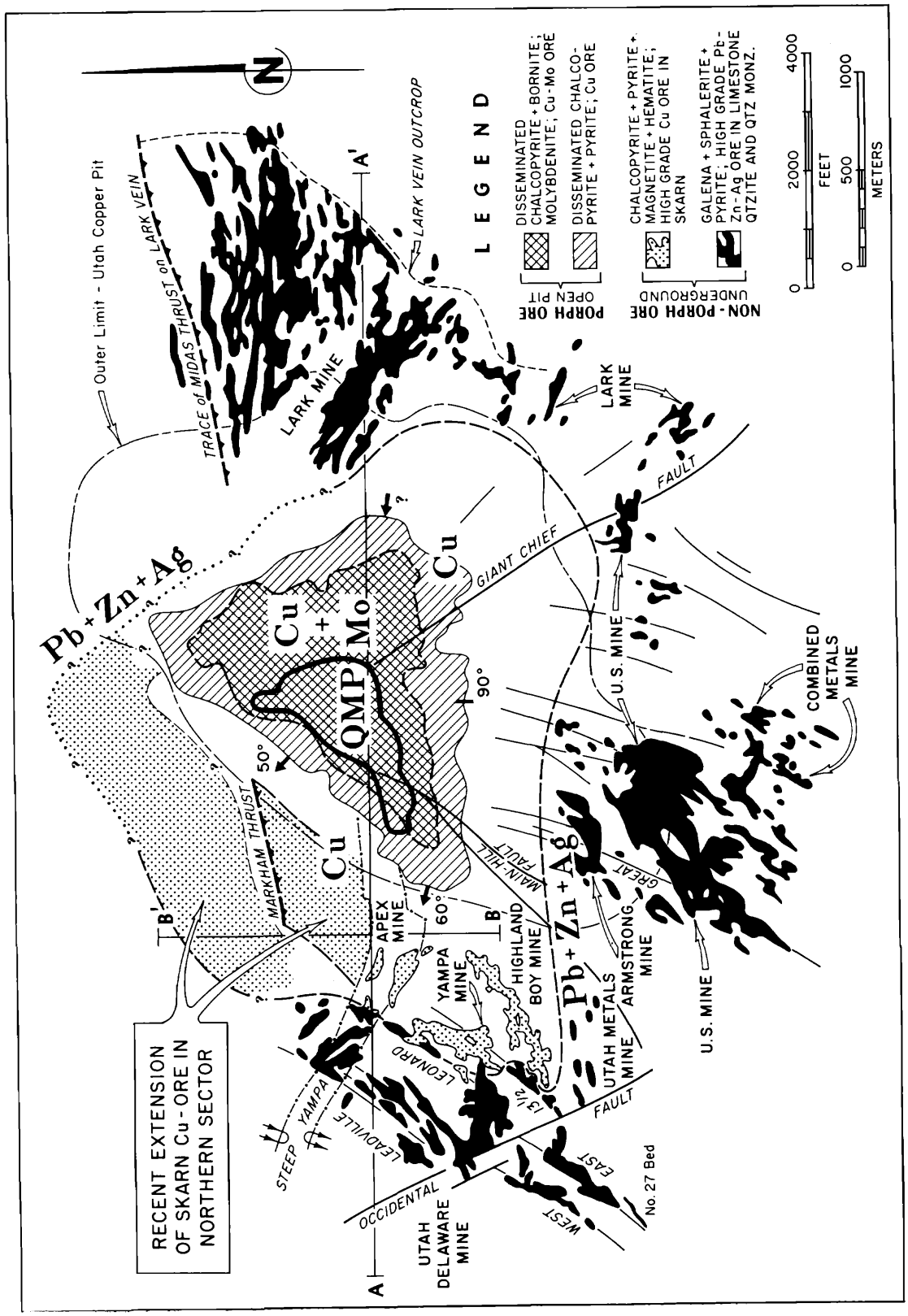

FIG. 17. Principal mines, surface projection of composite stoping, and metal zoning in the Bingham district. Porphyry ore zoning based on figure F-3 of John (1975); U. S. and Lark mines stoping based on Figure 1 of Rubright and Hart (1968). QMP = quartz monzonite porphyry.

skarn, chlorite is less common; locally it replaced garnet and diopside.

Montmorillonoids

Montmorillonoid clay is a common alteration product of diopside in the major limestone beds and in quartzite and is especially abundant near the stock and the present surface, where it occurs along fractures and Late Stage pyritic veins. Moderate to intense montmorillonoid alteration is pervasive in the low-grade copper zone adjacent to the stock at depth. The clay is commonly light to dark blue green in fresh core but changes to brown in a few hours or days. This rapid color change suggests a high ferrous iron content similar to the ferrosaponite described by Kohyama et al. (1973). A similar gray-brown clay occurs in garnet, but it is much less common. Actinolite also is altered to a clay, but in some instances actinolite appears to have coexisted stably with clay whereas adjacent diopside was altered.

All the above clays have a sharp (001) peak and a (060) spacing of about 1.54A. The latter spacing is indicative of the trioctahedral montmorillonoids, saponite or ferrosaponite. It is possible that the clay in garnet contains ferric iron and is nontronite rather than ferrosaponite. The (060) spacing for nontronite is about 1.53A, and poor quality peaks may have precluded this distinction.

Hunt (1957) studied alteration products in the U. S. mine and found light-colored saponite alteration of diopside adjacent to Pb-Zn-Ag fissures. Stringham and Taylor (1950) found nontronite alteration of tremolite and pyrophyllite in the Utah Copper pit adjacent to limonite veins. The nontronite was thought to have a supergene origin, but its described occurrence resembles that of clays in the Carr Fork area and it may belong to the Late Stage of alteration.

In the Highland Boy mine area, massive patches or streaks of gray to white waxlike clay were encountered in some drill core; this clay appears to be a direct replacement of marble rather than an alteration of silicates. X-ray studies indicate that this clay consists of halloysite, montmorillonite (060 = 1.49A), and some saponite. Winchell (1918) described a blue-green mineral which oxidized rapidly to brown from the Highland Boy mine; he named it "racewinite," although the description and analysis indicate that it is an iron-bearing aluminous montmorillonite.

Talc

Talc is common in small amounts as an apparent alteration product of actinolite-diopside. It usually occurs at the base of major skarn beds in areas of abundant sulfides. The most common association is talc-magnetite with tremolite, actinolite, or calcite. In one drill hole, talc occurs with calcite, magnetite, and serpentine at the base of the garnetized Highland Boy limestone. One meter deeper, X-ray results from one sample show that talc, calcite, and quartz accompany pyrite, chalcocite, digenite, bornite, tennantite, chalcopyrite, enargite, and aikenite ($PbCuBiSi_3$). These minerals do not represent an equilibrium assemblage, but the association of high-sulfur sulfides with talc suggests a hydrogen-metasomatizing environment similar to that represented by advanced argillic assemblages in aluminous rocks (Meyer and Hemley, 1967).

Gold mineralization

Garnetized limestone containing ore-grade copper mineralization generally averages 0.05 oz Au/ton. Higher gold assays, from 0.1 to 2.3 oz/ton and averaging about 0.2 oz/ton, occur locally in silicified and pyritized skarn. Veins of coarse-grained pyrite are common in such occurrences; garnet is replaced by quartz, very fine grained pyrite and local siderite; chalcopyrite is replaced by tennantite. Copper grade remains essentially constant from garnet through silicified and pyritized rock. Bordering the zones of silicified skarn, where relict garnet is still preserved, diopside is pervasively altered to clay.

District Zoning

The districtwide zonation of ores and alteration in the sedimentary wall rocks of the Bingham stock was first documented by R. N. Hunt in 1924: copper ores are restricted to intensely silicated limestone beds close to the intrusion, whereas lead-zinc-silver ores occur principally in limestone outside the zone of skarn minerals (Fig. 17). The apparent concentricity of metal zoning and its relation to the gross alteration features might suggest that the pattern is the result of contemporaneous zonal development related to progressive physicochemical changes in the ore fluid. However, although these relations are typically difficult to evaluate, a contemporaneous zonal growth model is untenable.

The present pattern may best be explained in terms of superimposed stages, although within a given stage a continuous process of zonal growth may be recognized. For example, during Main Stage copper sulfide deposition in quartzite and hornfels, biotite replaced actinolite near the stock, and actinolite replaced diopside farther out; these zones expanded outward with time and may well have been contemporaneous with development of andradite-magnetite-chalcopyrite in skarn and biotite-orthoclase-chalcopyrite in the stock. However, during the Late Stage, the retrograde clay-pyrite overprint crosscut these earlier zonal patterns. The bulk of the clay-

TABLE 7. Grade and Metal Ratios of Some Nonporphyry Ore from Carr Fork and the Lark Mine

Ft elevation	Wt % Cu	Oz/ton Au	Oz/ton Ag	Wt % Pb	Wt % Zn	Pb/Cu	Pb/Zn	Ag/Pb
Cristall fissure, Yampa limestone								
6770	0.7	0.04	6.4	13.4	NA	19.1	—	0.48
Leadville fissure, Highland Boy limestone								
6600	0.5	0.05	5	11	8	22.0	1.4	0.45
6600–6450	NA	0.04	5	13	13	—	1.0	0.38
6450–6350	NA	0.05	5	13	11	—	1.2	0.38
6350–6250	1.1	0.05	6	19	NA	17.3	—	0.32
6250–6150	1.4	0.04	5	14	NA	10.0	—	0.36
5530–5333	4.6	NA	3.3	2.4	NA	0.52	—	1.4
5333–5125	4.1	NA	NA	0.6	NA	0.15	—	—
5125–4930	1.8	NA	NA	0.4	NA	0.22	—	—
Leadville fissure, Yampa limestone								
4926	2.6	NA	NA	NA	NA	—	—	—
4926–4726	1.0	NA	NA	7.5	NA	7.5	—	—
4726–4522	NA	NA	NA	5.5	3.0	—	1.8	—
4326	2.4	0.06	2.1	NA	NA	—	—	—
Leonard (L) & Leeward Leonard (LL) fissures, Yampa								
7255–7090L	1.0	0.05	3.0	14	NA	14.0	—	0.21
5130 L	1.6	NA	NA	3.7	NA	3.1	—	—
5030 LL	2.8	NA	NA	7.5	12	2.7	0.63	—
4926 L	2.4	NA	NA	1.5	NA	0.63	—	—
4926 LL	4.1	0.15	2.4	NA	NA	—	—	—
4726 L				12.3	9.8	—	1.3	—
4726 LL	2.7	0.04	2.7	NA	NA	—	—	—
4522 L	NA	NA	NA	7	10	—	0.70	—
4426 L	NA	NA	NA	8.2	11.1	—	0.74	—
4326 L	NA	0.03	4.0	14	13	—	1.1	0.29
4326 LL	2.6	0.12	1.1	0.9	NA	0.35	—	1.2
West End Yampa footwall vein								
4522	2.2	0.02	0.7	0.95	NA	0.43	—	0.74
#27 Bed, west of Occidental fault								
6985	0.4	0.08	22.1	11.1	3.4	27.8	3.3	2.0
13½ fissure, Highland Boy limestone								
7300–6800	1.1	0.05	3.6	17.6	NA	16.0	—	0.20
Lark mine, concordant ore								
7000–4300	0.79	0.023	3.67	11.9	7.6	15.1	1.6	0.31
Lark mine, replacement ore								
?	0.55	0.035	4.39	12.2	9.3	22.2	1.3	0.36
Highland Boy mine skarn, Highland Boy limestone								
7255–6700	2.52	0.11	0.93	NA	NA	—	—	—
6700–6600	2.24	0.05	0.70	NA	NA	—	—	—
6600–6300	1.96	0.04	0.44	NA	NA	—	—	—
Average wollastonite zone, Yampa limestone outcrop								
7400–6850	0.0014	NA	0.043	0.021	0.046	15.0	0.46	2.0
Average garnet zone, Yampa limestone outcrop								
6600–6000	0.66	NA	0.15	0.003	0.023	0.02	0.13	50

Data from Lark based on Rubright and Hart (1968, tables III and IV).
Data on Yampa outcrop from Reid (1975, figs. 1–4).
NA = Not analyzed.
See Figures 2 and 3 for locations of fissures.

pyrite alteration of skarn and hornfels occurred along the contact with the stock at higher elevations, where late fracture density was highest. It appears to correspond temporally and spatially with the northeast-trending zone of late sericitic alteration in the western portion of the Bingham stock. The contemporaneity of clay-pyrite alteration in sedimentary rocks and sericitic alteration in igneous rocks has been pointed out before by J. P. Hunt (1957): in the U. S. mine lead-zinc veins in diopside-wollaston-

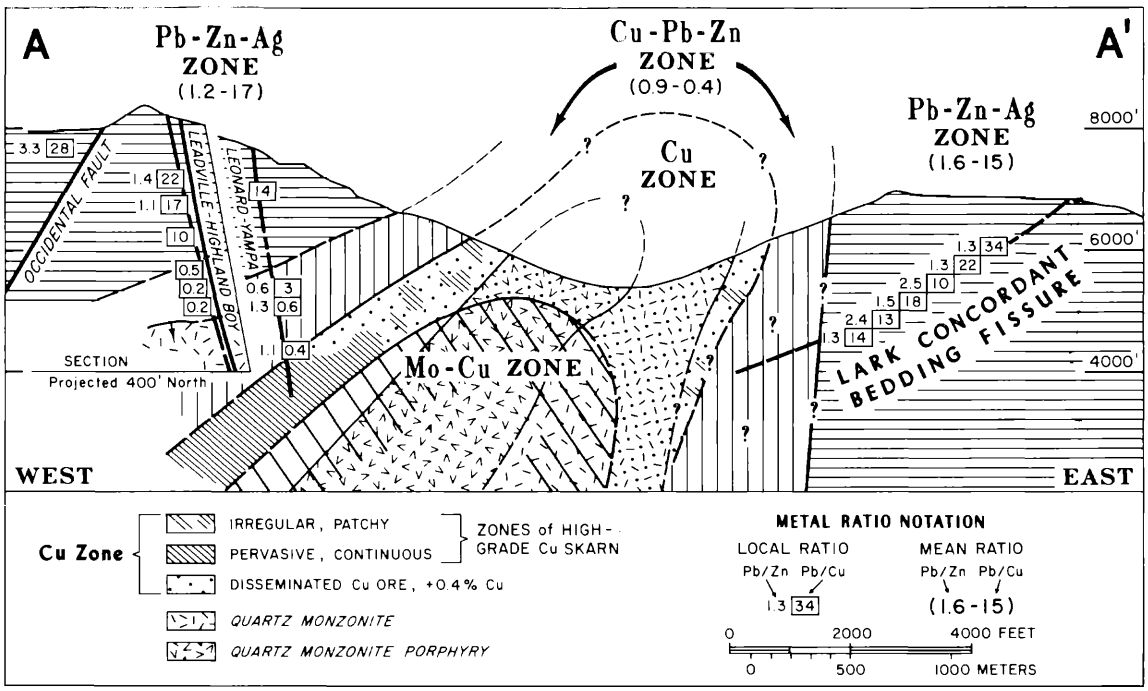

FIG. 18. East-west cross section located 120 m south of Apex shaft (see Fig. 2) illustrating metal zoning in the Bingham district. Data on west are projected up to 500 m from intersection of fissures with north-dipping limestone beds. Eastern portion of disseminated Cu zone based on John (1975); Lark concordant ore data based on Rubright and Hart (1968).

ite rock are surrounded by halos of talc and saponite, and similar veins in quartz monzonite of the Last Chance stock are surrounded by halos of sericite. In terms of the overall district pattern in sedimentary rocks, Hunt concluded that whereas copper mineralization may have been essentially contemporaneous with skarn development, much lead-zinc mineralization was associated with a hydrogen-metasomatizing environment superimposed on earlier skarn (in Meyer and Hemley, 1967, p. 195).

Additional data bearing on zoning of Late Stage mineralization and its relation to the Main Stage of copper mineralization are presented below.

Metal ratios: Metal zoning data for fissure and concordant bedding ore are summarized in Table 7 and Figure 18. Metal ratios for the western sector in Figure 18 are based on production and assay data for Leadville fissure ore in the Highland Boy limestone and Leonard fissure ore in the Yampa limestone. The large and systematic changes in the Pb/Cu ratio make it the single most useful zoning index (c.f. Goodell and Petersen, 1974).

The data for the western sector clearly indicate a zonation with depth in the fissures from lead-zinc-silver ore, characterized by Pb/Cu = 10 to 25, to copper-lead-zinc and copper-lead ore, characterized by Pb/Cu = 0.1 to 0.5, over a vertical range of 880 m. Copper-lead-zinc ore extends to the quartz monzonite contact in the Leadville fissure ore of the Highland Boy limestone. Farther north, where the porphyry is in direct contact with sedimentary rocks, a zone up to 300 m wide and subparallel with the porphyry contact contains all of the major occurrences of copper ore in silicated limestone. These ores are characterized by Pb/Cu < 0.05. The copper zone is interpreted in Figure 18 (compare with Fig. 15) as the downward extension of the bornite-chalcopyrite and chalcopyrite-pyrite zones of the porphyry mineralization pattern defined by James (1971) and John (1975). At depths below 5,000-ft elevation, a downward-widening zone of low copper grades in sedimentary rocks separates the skarn copper ore from the porphyry, which itself is essentially barren of copper but contains significant molybdenite. This low-grade skarn zone is interpreted as a part of the molybdenite zone and barren core zone of the porphyry mineralization pattern defined by James (1971) and John (1975).

In the Carr Fork area, lead-zinc-silver and copper-lead fissure-replacement ore generally occurs closer to the surface and west of the copper-bearing skarn. However, lead-zinc-silver ore is locally superimposed on copper ore and no copper-lead ore is present. For example, the Yampa limestone between 6,570- and 7,073-ft elevation contains lead-zinc-silver ore in northeast fissures (Leonard vein) and bedding fis-

sures (Craig vein) near the hanging wall, whereas pyritic copper ore occurs in bedding fissures near the footwall and extends west of the lead fissures as much as 60 m (Upper Yampa copper stopes). Available information does not reveal the presence of copper-lead mineralization in this area; assays from one lead stope indicate a Pb/Cu ratio of 14, which is characteristic of the outer lead-zinc-silver zone. At the western end of the Highland Boy mine, copper stopes give way to lead stopes. However, all of the lead mineralization is related to the 13½ fissure system and is not a contemporaneous part of the copper-bearing skarn assemblage. Although copper and lead stopes are intermingled in this area, Pb/Cu ratios in individual lead stopes are all between 10 and 22, values characteristic of the outer lead-zinc-silver zone.

Metal ratios for the Lark area on the east side of the district are based on the average grade of ore from one of the major concordant orebodies which extends over a vertical range of 800 m at an average dip of 38° WNW (Rubright and Hart, 1968, table III). Each datum point in Figure 18 represents the average of two mine levels. The vertical range is comparable to that of zoned fissures in the western sector, yet this eastern sector orebody displays no zoning. Although the *grades* are erratic in the eastern sector, the *ratios* display little variation and clearly are comparable to lead-zinc-silver ores of the western sector above 6,000-ft elevation.

The published record on occurrences of copper ore in the Lark and U. S. mines is meager. Stopes with high copper content are present in the eastern portion of the U. S. mine, but these also contain high lead (Rubright and Hart, 1968); the Pb/Cu ratio for one such stope for which grades are available is 30. The apparent lack of copper-bearing skarn on the eastern and southern contact zones of the porphyry is due to the fact that the wall rock in these areas consists of quartz monzonite; the downward continuation of the porphyry copper ore zone is contained largely within the quartz monzonite rather than in limestone skarns as in the western and northern sectors.

The metal zoning pattern illustrated in Figure 18 suggests that if the axis of the pattern were originally vertical, then the Bingham district is tilted to the east approximately 25 degrees. Such a tilt, presumably caused by Basin and Range faulting, is also suggested by the attitude of pyroclastic rocks on the eastern range front (Smith, 1961).

The above-cited evidence for changes in the character of mineralization with time is consistent with the concept of complex fluid convective patterns associated with repeated surges of magmatic fluids and mixing with meteoric waters suggested by Roedder (1971) and Moore and Nash (1974). The influx of meteoric waters which brought about the local, veinlet-related, sericitic alteration of early K-feldspar + biotite assemblages in the intrusive rocks of the Bingham stock may well have been essentially contemporaneous with the Late Stage encroachment of peripheral lead-zinc-silver and lead-copper mineralization onto the inner skarn zones.

Summary and Conclusions

The geometry of folding and faulting had an important influence on the configuration of the Bingham stock and the distribution of related ores. Following the main period of folding and bedding plane slippage, continued deformation resulted in local overturning of beds, northward thrusting on west-northwest-striking faults and right-lateral offset on northwest-striking faults. The west portion of the district displays a greater degree of shortening than the eastern portion.

Sedimentary rocks in the Carr Fork area originally consisted primarily of variable mixtures of calcite and quartz; the original calcite: quartz ratio exerted an important influence on the mineralogical compositions of rocks undergoing magnesium and iron metasomatism and copper deposition.

Initially, calcite in quartzite and thin silty limestones was replaced by talc, then tremolite, and finally by diopside. On the western contact of the Bingham stock the evidence suggests that the diopside zone in quartzite predates garnetization of the wollastonite zone in limestones. Thus, diopside formation may be related to the early stages of quartz monzonite porphyry emplacement, or it may be contemporaneous in part with quartz monzonite emplacement and the formation of the district-wide wollastonite zone. The definition of the districtwide pattern of Mg metasomatism remains an important aspect for future research.

Subsequently, diopside in quartzite and interbedded, thin silty limestone was altered to actinolite and biotite in a zone of sulfide veinlets near the intrusion. Toward the intrusion, (1) the ratio of chalcopyrite to pyrite gradually increases, (2) the abundance of molybdenite-bearing veinlets increases, (3) the total sulfide content increases to a maximum, then decreases, and (4) the intensity of actinolite and biotite alteration associated with sulfides increases. These patterns of mineralization and alteration represent Main Stage zones which expanded outward with time. Veinlets at the contact with the stock indicate that the Main Stage was in part contemporaneous with sulfide veining and biotite-orthoclase alteration of quartz monzonite.

A zone up to 60 m wide in the sedimentary rocks along the porphyry contact contains less than 0.1

percent sulfides, principally pyrite. Diopside hornfels is nearly pervasively altered to montmorillonoid clays, whereas biotite remains stable in the more siliceous sediments. The alteration and sulfide assemblages are similar to those in the adjacent porphyry.

The two major limestones, the Highland Boy and the Yampa, also consisted originally of calcite and quartz. Early Stage decarbonation and silication produced a wollastonite-bearing calcite marble, which was locally replaced by a fine-grained diopside-calcite mixture with an erratic distribution. Later, during the Main Stage, formation of iron-rich garnet proceeding along steep fractures and then along marble layers, finally replacing intervening wollastonite layers. An estimated one-third of the copper deposited in silicated limestone accompanied garnet; a common favorable site of deposition is the interface between garnet and diopside. Massive, pure magnetite replaced garnet adjacent to the stock at lower elevations. At higher elevations the skarns have a lower average iron oxide content, and specular hematite is as abundant as magnetite.

Replacement of diopside-quartz hornfels and quartzite by actinolite and sulfides, and replacement of wollastonite-calcite rock by andradite, magnetite, and sulfides, occurred during a wave of iron metasomatism that moved out from the stock contact. This contrasting mineralogy associated with Main Stage sulfide deposition largely was controlled by differences in the calcium : magnesium ratio of individual beds. Actinolite may have continued to form in both environments as temperatures dropped toward facies B and C (Fig. 14) : iron-bearing diopside in skarn was altered to quartz-actinolite-magnetite, associated with relict garnet. At still lower tempreatures, garnet was altered to quartz and calcite associated with one or more of the iron-bearing minerals magnetite, hematite, chalcopyrite, pyrite, and siderite. Roughly two-thirds of the chalcopyrite in skarn and the highest grade of copper occurs with these alteration products of diopside and garnet.

A Late Stage of argillic alteration produced pyrite, chlorite, montmorillonoids, sericite, and talc from early calc-silicates. This alteration is especially pervasive in a zone up to 60 m wide near the intrusive contact, where northeast-striking faults may have channelized late fluids. Copper appears to have been redistributed only during the Late Stage; sulfide assemblages contain a higher proportion of pyrite than Main Stage assemblages and magnetite and hematite are absent. Relatively high gold values accompany a part of the Late alteration characterized by pyritization and silicification of calc-silicates and replacement of chalcopyrite by tennantite.

In contrast with lead-zinc-silver mineralization, which displays abrupt assay boundaries, copper mineralization outside the high-grade skarn is broad and diffuse. The pattern of highest copper grade for any given rock type displays the typical steep-sided, dome-shaped configuration of mineralization associated with porphyry copper intrusives. Near its probable upper limit the pattern was approximately 1,200 m in diameter, whereas at depths approaching 3,000 m below its uppermost extent the pattern is approximately 2,500 m in diameter. The overall depth of the copper zone is unknown, but on the western contact high-grade skarn extends below the 1,400-ft elevation. This indicates the presence of an original vertical column of ore-grade mineralization in excess of 3,300 m.

A general time framework for the zonal development of alteration and mineralization in limestone can be established on the basis of available data. The presence of sparse disseminated sphalerite and galena in the outer wollastonite zone suggests that a very minor amount of lead-zinc mineralization occurred in a fringe position and perhaps early relative to copper ore associated with garnetization. However, the major lead-zinc-silver ores in part cut and alter wollastonite and garnet, and hence are clearly later than silication at any given point in the pattern. The relative timing of copper to lead-zinc on a district scale is indeterminate, however. It is possible, for example, that as the skarn and its attendant copper mineralization was forming near the intrusion, lead-zinc ores were being deposited farther out in fresh limestone. Then, as the system cooled and as the inner part of the aureole suffered Late alteration, fluids responsible for lead-zinc mineralization in the outer zones encroached back into the skarn zones.

In conclusion, the following sequence of events is offered as a general model of the process of formation of ores in the Bingham district: Moore (1973) has shown that the changes in composition of a series of intrusive and extrusive rocks in the Bingham district indicates a period of 9 m.y. of progressive differentiation. Presumably, this led to saturation with respect to volatiles at the time of intrusion of the Bingham quartz monzonite porphyry. The porphyry intruded the earlier quartz monzonite and sedimentary rocks, mineralizing them essentially simultaneously. The addition of S, Cu, Fe, Mg, K, H, and minor Al formed a zoned skarn whose mineralogy depended on the original bulk composition of the sedimentary rocks and distance from the intrusive contact. The development of actinolite alteration in quartzite and of andradite in limestone occurred during potassic alteration of the Bingham stock and represents a major period of copper sulfide deposi-

tion. After the porphyry solidified, copper and other elements continued to be introduced or redistributed as a consequence of the loss of heat and volatiles. Andradite was altered to calcite-quartz-iron oxide and actinolite-bearing assemblages, presumably during the end stage of potassic alteration in the stock and actinolite alteration in quartzite. Chloritic, argillic, and sericitic alteration in sedimentary rocks, as well as lead-zinc and gold deposits, may have formed during the late convective entry of ground water which led to sericitization in the stock.

Acknowledgments

The present study is a direct result of interpretations of data gathered during the exploration and definition of a major ore zone in the Carr Fork area by the Anaconda Company; we wish to express our appreciation to the officers of the company for permission to publish this paper. The writers are indebted to many others who have contributed to the study: John P. Hunt had the vision to take a new approach at Carr Fork and provided us with the enthusiastic support to carry it out. The project owes much of its success to this determination to apply scientific methods to exploration. We have benefited from discussions with former colleagues, particularly W. J. Garmoe and J. J. Hemley. M. A. Haddadin and Hossein Salek provided invaluable aid with mineralogical determinations. Chemical analyses were carried out by James Cardwell and H. A. Vincent. The figures were drafted by David Severson. We also wish to express our appreciation to the many geologists who previously mapped the underground mines and logged drill core at Carr Fork, thus providing much of the background upon which recent drilling was based. D. M. Burt, Allan H. James, and T. G. Theodore reviewed earlier versions of the manuscript.

W. W. A., JR.
DEPARTMENT OF GEOLOGICAL SCIENCES
UNIVERSITY OF COLORADO
BOULDER, COLORADO 80309
M. T. E.
DEPARTMENT OF APPLIED EARTH SCIENCES
STANFORD UNIVERSITY
STANFORD, CALIFORNIA 94305
May 23, 1978

REFERENCES

Atkinson, W. W., Jr., 1975, Alteration and mineralization in surface exposures at Carr Fork, Bingham district, Utah, *in* Bray, R. E., and Wilson, J. C., eds., Guide Book to the Bingham mining district, Soc. Econ. Geologists, October 23, 1975: Bingham Canyon, Utah, Kennecott Copper Corp., p. 119–133.

—— 1976, Zoning and paragenesis of ores in the San Pedro Mountains, *in* Woodward, L. A., and Northrop, S. A., eds., Tectonics and mineral resources of southwestern North America: New Mexico Geol. Soc. Spec. Pub. 6, p. 187–191.

Boutwell, J. M., 1905, Economic geology of the Bingham mining district, Utah: U. S. Geol. Survey Prof. Paper 38, 413 p.

Bray, R. E., 1969, Igneous rocks and hydrothermal alteration at Bingham, Utah: ECON. GEOL., v. 64, p. 34–49.

Burt, D. M., 1972, Mineralogy and geochemistry of Ca-Fe-Si skarn deposits: Unpub. Ph.D. thesis, Harvard University, Cambridge, Mass., 256 p.

Butler, B. S., Loughlin, G. S., Heikes, V. C., and others, 1920, The ore deposits of Utah: U. S. Geol. Survey Prof. Paper 111, 672 p.

Deer, W. A., Howie, R. A., and Zussman, J., 1966, An introduction to the rock-forming minerals: New York, John Wiley and Sons, Inc., 528 p.

Einaudi, M. T., 1975a, Iron metasomatism of sedimentary rocks near the Bingham stock, *in* Bray, R. E., and Wilson, J. C., eds., Guide Book to the Bingham mining district, Soc. Econ. Geologists, October 23, 1975: Bingham Canyon, Utah, Kennecott Copper Corp., p. 135–139.

—— 1975b, Graphical analysis of some skarn assemblages in the system Ca-Fe-Mg-Si-H_2O-CO_2-O_2 [abs.]: EOS, v. 56, p. 1081.

Farmin, Rollin, 1933, Influence of Basin-Range faulting in mines at Bingham, Utah: ECON. GEOL., v. 28, p. 601–606.

Field, C. W., 1966, Sulfur isotope abundance data, Bingham district, Utah: ECON. GEOL., v. 61, p. 850–871.

Field, C. W., and Moore, W. J., 1971, Sulfur isotope study of the "B" limestone and Galena fissure ore deposits of the U. S. mine, Bingham mining district, Utah: ECON. GEOL., v. 66, p. 48–62.

Gilluly, James, 1932, Geology and ore deposits of the Stockton and Fairfield quadrangles, Utah: U. S. Geol. Survey Prof. Paper 173, 171 p.

Goodell, P. C., and Petersen, Ulrich, 1974, Julcani mining district, Peru: a study of metal ratios: ECON. GEOL., v. 69, p. 347–361.

Gustafson, W. I., 1974, The stability of andradite, hedenbergite and related minerals in the system Ca-Fe-Si-O-H: Jour. Petrology, v. 15, p. 455–496.

Hunt, J. P., 1957, Rock alteration, mica, and clay minerals in certain areas in the United States and Lark mines, Bingham, Utah: Unpub. Ph.D. thesis, Univ. California Berkeley, 321 p.

Hunt, R. N., 1924, The ores in limestones at Bingham, Utah: Am. Inst. Mining Metall. Engineers Trans., v. 70, p. 856–883.

—— 1933, Bingham mining district: Internat. Geol. Cong., 16th, Guidebook 17, p. 45–56.

James, A. H., 1971, Hypothetical diagrams of several porphyry copper deposits: ECON. GEOL., v. 66, p. 43–47.

James, A. H., Smith, W. H., and Bray, R. E., 1961, The Bingham district—a zoned porphyry ore deposit, *in* Cook, D. R., ed., Geology of the Bingham mining district and northern Oquirrh Mountains: Utah Geol. Soc. Guidebook 16, p. 81–100.

James, A. H., Smith, W. H., and Welsh, J. E., 1961, General geology and structure of the Bingham district, Utah, *in* Cook, D. R., ed., Geology of the Bingham mining district and northern Oquirrh Mountains: Utah Geol. Soc. Guidebook 16, p. 49–71.

John, E. C., 1975, Mineral zones of the Bingham district, *in* Bray, R. E., and Wilson, J. C., eds., Guide Book to the Bingham mining district, Soc. Econ. Geologists, October 23, 1975: Bingham Canyon, Utah, Kennecott Copper Corp., p. 59–72.

Kohyama, Norihiko, Shimoda, Susumu, and Sudo, Toshio, 1973, Iron-rich saponite (ferrous and ferric forms): Clays and Clay Minerals, v. 21, p. 229–237.

Lanier, George, Folsom, R. B., and Cone, S., 1975, Alteration of equigranular quartz monzonite, Bingham District, Utah: *in* Bray, R. E., and Wilson, J. C., eds., Guide Book to the Bingham mining district, Soc. Econ. Geologists, October 23, 1975: Bingham Canyon, Utah, Kennecott Copper Corp., p. 73–97.

Lindgren, Waldemar, 1924, Contact metamorphism at Bingham, Utah: Geol. Soc. America Bull., v. 35, p. 507–534.

Lowell, J. D., and Guilbert, J. M., 1970, Lateral and vertical

alteration-mineralization zoning in porphyry ore deposits: ECON. GEOL., v. 65, p. 373–408.
Meyer, Charles, and Hemley, J. J., 1967, Wall rock alteration, *in* Barnes, H. L., ed., Geochemistry of hydrothermal ore deposits: New York, Holt, Rinehart and Winston, p. 166–235.
Moore, W. J., 1973, Igneous rocks in the Bingham mining district, Utah: U. S. Geol. Survey Prof. Paper 629-B, 42 p.
Moore, W. J., and Czamanske, G. K., 1973, Compositions of biotites from unaltered and altered monzonitic rocks in the Bingham mining district, Utah: ECON. GEOL., v. 68, p. 269–274.
Moore, W. J., and Nash, J. T., 1974, Alteration and fluid inclusion studies of the porphyry copper ore body at Bingham, Utah: ECON. GEOL., v. 69, p. 631–645.
Morgan, B. A., 1975, Mineralogy and origin of skarn in the Mount Morrison pendant, Sierra Nevada, California: Am. Jour. Sci., v. 275, p. 119–142.
Nielsen, R. L., 1970, Mineralization and alteration in calcareous rocks near the Santa Rita stock, New Mexico: New Mexico Geol. Soc. 21st Field Conf., p. 133–139.
Reid, Julia, 1975, Skarn alteration of the Commercial limestone in the Carr Fork area, *in* Bray, R. E., and Wilson, J. C., eds., Guide Book to the Bingham mining district, Soc. Econ. Geologists, October 23, 1975: Bingham Canyon, Utah, Kennecott Copper Corp., p. 105–118.
Rickwood, P. C., 1968, On recasting analyses of garnet into end-number molecules: Contr. Mineralogy Petrology, v. 18, p. 175–198.
Roberts, R. J., and Tooker, E. W., 1961, Structural geology of the north end of the Oquirrh Mountains, *in* Cook, D. R., ed., Geology of the Bingham mining district and northern Oquirrh Mountains: Utah Geol. Soc. Guidebook 16, p. 36–48.
Roberts, R. J., Crittenden, M. D., Jr., Tooker, E. W., Morris, H. T., Hose, R. K., and Cheney, T. M., 1965, Pennsylvanian and Permian basins in northwestern Utah, northeastern Nevada, and south-central Idaho: Am. Assoc. Petroleum Geologists Bull., v. 49, p. 1926–1956.
Roedder, Edwin, 1971, Fluid inclusion studies on the porphyry-type ore deposits at Bingham, Utah, Butte, Montana, and Climax, Colorado: ECON. GEOL., v. 66, p. 98–120.
Rubright, R. D., and Hart, O. J., 1968, Non-porphyry ores of the Bingham district, Utah, *in* Ridge, J. D., ed., Ore deposits of the United States, 1933–67 (Graton-Sales vol.): New York, AIME, v. 1, p. 886–907.
Slaughter, J., Kerrick, D. M., and Wall, V. J., 1975, Experimental and thermodynamic study of equilibria in the system CaO-MgO-SiO_2-H_2O-CO_2: Am. Jour. Sci., v. 275, p. 143–162.
Smith, W. H., 1961, The volcanics of the eastern slopes of the Bingham district, Utah, *in* Cook, D. R., ed., Geology of the Bingham mining district and northern Oquirrh Mountains: Utah Geol. Soc. Guidebook 16, p. 101–119.
—— 1975, General structural geology of the Bingham mining district, *in* Bray, R. E., and Wilson, J. C., eds., Guide Book to the Bingham mining district, Soc. Econ. Geologists, October 23, 1975: Bingham Canyon, Utah, Kennecott Copper Corp., p. 41–48.
Stacey, J. S., Moore, W. J., and Rubright, R. D., 1967, Precision measurement of lead isotope ratios; preliminary analyses from the U. S. mine, Bingham Canyon, Utah: Earth Planet. Sci. Letters, v. 2, p. 489–499.
Stewart, J. H., Moore, W. J., and Zietz, Isidore, 1977, East-west patterns of Cenozoic igneous rocks, aeromagnetic anomalies, and mineral deposits, Nevada and Utah: Geol. Soc. America Bull., v. 88, p. 67–77.
Stringham, B. F., 1953, Granitization and hydrothermal alteration at Bingham, Utah: Geol. Soc. America Bull., v. 64, p. 945–991.
Stringham, B. F., and Taylor, Allen, 1950, Nontronite at Bingham, Utah: Am. Mineralogist, v. 35, p. 1060–1066.
Tooker, E. W., 1970, Radial movements in the western Wyoming salient of the Cordilleran overthrust belt: discussion: Geol. Soc. America Bull., v. 81, p. 3503–3506.
—— 1971, Regional structural controls of ore deposits, Bingham mining district, Utah, U. S. A.: Geol. Soc. Japan Spec. Issue 3 (Proc. IMA-IAGOD meetings, IAGOD vol.), p. 76–81.
Tooker, E. W., and Roberts, R. J., 1962, Comparison of Oquirrh Formation sections in the northern and central Oquirrh Mountains, Utah, *in* Geological Survey research 1962: U. S. Geol. Survey Prof. Paper 450-E, p. E32-E36.
Winchell, A. N., 1918, Racewinite: A peculiar mineral from ore deposits in Utah: ECON. GEOL., v. 13, p. 611–615.
—— 1924, Petrographic studies of limestone alterations at Bingham: Am. Inst. Mining Metall. Engineers Trans., v. 70, p. 884–889.
Zietz, Isidore, Bateman, P. C., Case, J. E., Crittenden, M. D., Jr., Griscom, A., King, E. R., Roberts, R. J., and Lorentzen, G. R., 1969, Aeromagnetic investigation of crustal structure for a strip across the western United States: Geol. Soc. America Bull., v. 80, p. 1703–1714.